



# Large Diameter Piles Under Lateral Loading – A Database Study

**Yen-Chih Wang**, Research Assistant, Texas A&M University, College Station, TX, U.S.A.; email: [wmark107@tamu.edu](mailto:wmark107@tamu.edu)

**Jean-Louis Briaud**, Distinguished Professor, Texas A&M University, College Station, TX, U.S.A.; email: [briaud@tamu.edu](mailto:briaud@tamu.edu)

**ABSTRACT:** The question to be answered is: how well are current  $P-y$  curves predicting the behavior of large diameter piles subjected to monotonic lateral loading? Current  $P-y$  curves were developed about 60 years ago based on lateral load tests on piles which ranged from 0.3 to 0.6 m in diameter. Today's pile diameters can reach 4 m or more. This significant difference in scale brings into question the applicability of these early  $P-y$  curves to today's large diameter piles. A horizontal load tests database of 46 piles with diameters larger than 1.5 m (up to 3.0 m) and 64 piles with diameters less than 1.5 m both in sand and in clay was assembled. Predictions of load and displacement were carried out using commonly used  $P-y$  curves and the software LPILE. Within this paper, these predictions are compared to the measured loads and measured displacements. The ratio of predicted over measured quantities is plotted against pile diameter, and trends are noted. Modifications to the  $P-y$  curves are then proposed so that the ratio of predicted over measured displacement remains approximately independent of diameter. Finally, the probability that the predictions will be unsafe is evaluated.

**KEYWORDS:** piles, large diameter, load tests, database,  $P-y$  curves, deflection, lateral load, LPILE, probability.

**SITE LOCATION:** [Geo-Database](#)

## INTRODUCTION

The diameter of piles has increased steadily, from 0.3 to 0.6 m being typical some 60 years ago to diameters as large as 4 or 5 m being used today. This is due in part to a continuous increase in the size of our infrastructure elements, some of which are subjected to significant horizontal loading. There are several solutions to estimate the behavior of single piles subjected to horizontal loading. One of them consists of assuming that the soil can be represented by a series of individual non-linear springs and that the pile is made of corresponding elements. The governing differential equation is solved by the finite difference method and the design approach is known as the  $P-y$  curve analysis. This approach is credited to Matlock (1970) and later Reese et al. (1974). In their remarkable contribution, Matlock and Reese ran a series of horizontal load tests on 0.3 to 0.6 m diameter piles in soft clay, in sand, and in stiff clay to calibrate the  $P-y$  non-linear soil springs. Today's pile diameters have increased dramatically, ensuing in the question of whether the original  $P-y$  curves are still valid for large diameter piles. This is the subject of this paper.

The problem of a laterally loaded pile has been under investigation for some time, and various  $P-y$  curves have been proposed, including by Reese (1958, 1975), Matlock (1970), Randolph and Housby (1984), Jeanjean (2009), and Zhang et al. (2016). This project addresses the diameter effect from a database point of view while using the most common  $P-y$  curves. The computer program LPILE (Ensoft, 2018) is used to compare the predictions with the measurements collected from pile load tests. The  $P-y$  curves proposed by Matlock (1970) and Reese et al. (1975) in clay and Reese et al. (1974) which evolved into the American Petroleum Institute (API) (2010) recommendations in sand are used to make the predictions.

## THE DATABASE

A database of horizontal pile load tests was assembled (Table 1). It included small diameter piles (diameter  $B < 1.5$  m) and large diameter piles ( $B \geq 1.5$  m). More than 40 people were contacted in 9 countries, and 110 load tests were assembled,

Submitted: 15 July 2020; Published: 10 August 2021

Reference: Wang Y.C., Briaud J.L. (2021). Large Diameter Piles Under Lateral Loading – A Database Study.

International Journal of Geoengineering Case Histories, Volume 6, Issue 2, pp. 41-66, doi: 10.4417/IJGCH-06-02-03

including tests on 46 large diameter piles and 64 small diameter piles. The length of the piles varied from 0.76 m to 93.6 m and the aspect ratio L/B from 0.5 to 74. Details about each load test, including soil stratigraphy with soil properties, pile properties, and the applied lateral load versus pile head displacement curves, were organized in a large spreadsheet called TAMU-LATERAL, which is available upon request (Briaud & Wang, 2018).

*Table 1. TAMU-LATERAL Database: Major Features.*

| Category           | Small Diameter Pile | Large Diameter Pile    |
|--------------------|---------------------|------------------------|
|                    | $B < 1.5 \text{ m}$ | $B \geq 1.5 \text{ m}$ |
| Pile diameter (m)  | 0.15 – 1.5          | 1.5 – 3.0              |
| Pile length (m)    | 1.52 – 36.6         | 0.76 – 93.6            |
| Aspect Ratio (L/B) |                     | 0.5 - 74               |
| Number of cases    | 64                  | 46                     |
| Soil type          | Sand<br>Clay        | 33<br>30<br>16         |

The load tests came from 9 different countries and each test was given a Record Number (RN). The available data varied from one RN to the next. The following information can be found in the spreadsheet but not necessarily for each RN:

1. The lateral load  $H_o$  versus lateral deflection  $y_o$  near the groundline
2. The pile type (e.g., bored pile, steel pipe pile)
3. The pile geometry (e.g., diameter, length, wall thickness)
4. The pile properties (e.g., elastic modulus, moment of inertia)
5. The soil stratigraphy
6. The soil type (e.g., sand, clay, layer thickness, ground water table). The soil type was classified according to the dominant soil type within the top one third of the pile length below the ground surface. Sand sites and gravel sites were regrouped and called sand sites. Clay sites and silt sites were regrouped and called clay sites. There were 63 sand sites and 47 clay sites in the database.
7. The soil parameters (e.g., effective unit weight ( $\gamma$ ), friction angle ( $\phi$ ) for sand, undrained shear strength ( $s_u$ ) for clay, unconfined compressive strength for clay/rock ( $q_u$ ), normal strain at 50% of ultimate ( $\epsilon_{50}$ ), Standard Penetration Test blow count (N), plasticity index (PI), pressuremeter limit pressure ( $p_L$ ), pressuremeter modulus ( $E_o$ ), cone penetrometer point resistance ( $q_c$ ), and shear wave velocity ( $v_s$ )).

## P-y CURVE USED

The P-y curve approach to predict the behavior of laterally loaded piles is commonly used in practice. Other approaches include analogy methods (e.g., Briaud, 2013), elastic solutions (e.g., Poulos, 1971; Banerjee and Davies 1978; Randolph, 1981), finite element methods (e.g., Comodromos and Pitilakis, 2005; Byrne et al., 2015; Ahmed and Hawlader, 2016), force and moment equilibrium-based solutions (e.g., Brinch Hansen, 1961, Broms, 1964a and 1964b, Motta, 2012; Zhang and Ahmari, 2013), and the strain wedge model (e.g., Ashour et al., 2002).

The P-y curve method (e.g., McClelland, 1956; Matlock, 1970; Reese et al., 1975) is the method evaluated in this article. The pile is represented as an elastic member with a bending stiffness  $EI$  where  $E$  is the modulus of the pile material and  $I$  is the moment of inertia around the bending axis. The soil is represented by a series of nonlinear springs with depth; each nonlinear spring behavior is described by the P-y curve where  $P$  is the line load (kN/m) on an element of pile and  $y$  is the horizontal displacement of that pile element. The governing differential equation is based on equilibrium, on the constitutive model for the pile, and on the constitutive model for the soil which is the P-y curve. It is solved by the finite difference method.

The P-y curves used in this study were the Matlock (1970) P-y curve for soft clay, the Reese et al. (1975) P-y curve for stiff clay, and the API (RP2A, 2010) P-y curve for sand as an evolution of the Reese et al. (1974) P-y curve for sand. These P-y curves are described in detail in the publications cited above and in the LPILE (2018) manual. In clay, the main parameters required to develop the P-y curves are the undrained shear strength  $s_u$  and the normal strain  $\epsilon_{50}$  at 50% of the ultimate deviator stress in a triaxial test. In sand, the main parameters are the friction angle  $\phi$  and the horizontal modulus of subgrade reaction  $k$ . In layered soil profiles, different P-y curves can be used at different depths depending on the soil type encountered.

## ULTIMATE HORIZONTAL LOAD

For vertically loaded piles, it is common practice to calculate the ultimate vertical load. Yet this is not common practice for horizontally loaded piles. In this paper, the ultimate horizontal load  $H_{ou}$  is defined as the load corresponding to a lateral pile head displacement equal to one tenth of the pile diameter or width (B/10). In the TAMU-LATERAL database, some load tests were carried out past a pile head displacement of B/10, some close to B/10, and some that did not come close to approaching B/10 displacement value. Extrapolation was used when the load test did not reach B/10. The extrapolation was conducted by fitting a hyperbola to the top load vs. top displacement curve. If the pile top displacement was at least B/30, the extrapolation was considered reasonable, and if not, the extrapolation was considered unreasonable. Fig. 1 shows examples of such extrapolations. In Figure 1(a), the extrapolation is considered reasonable. In Figure 1(b), the extrapolation is considered unreasonable because fitting the measured data at small displacements with slightly different fitting models leads to very different  $H_{ou}$  values.

Table 2 gives a summary of the number of times the extrapolation was required, how often it was considered reasonable, and how often it was considered unreasonable according to the B/30 criterion. As can be seen in the end, it was possible to obtain  $H_{ou}$  with no extrapolation or reasonable extrapolation for 28 small piles (B<1.5m) in sand, 28 small piles in clay, 12 large piles (B>1.5m) in sand, and 6 large piles in clay. Therefore, the total number of piles for which  $H_{ou}$  could be determined was 74, with 56 small diameter piles and 18 large diameter piles. Furthermore, 5 of the small piles in sand were tapered piles for which defining the pile diameter was not straightforward, and so these 5 tapered piles were not considered in the final database. Knowledge of the ultimate load was necessary because, in a later part of the paper, the predicted and measured deflection will be compared at various percentages of the ultimate load. Knowledge of the ultimate lateral load was not necessary, however, for the other set of comparisons which were based on set values of the groundline deflection. To be consistent, the same number of load tests were nonetheless considered for both load and deflection evaluations. Ultimately, there were 23 small diameter piles in sand, 12 large diameter piles in sand, 28 small diameter piles in clay, and 6 large diameter piles in clay for a total of 69 piles.

The ultimate horizontal load  $H_{ou}$  can be estimated by (Briaud, 2013):

$$H_{ou} = 0.75 p_L B z_{max} \quad (1)$$

Where  $p_L$  is the pressuremeter limit pressure, B is the pile diameter or width, and  $z_{max}$  is the depth to the maximum bending moment. Briaud (2013) explains how to calculate  $z_{max}$ . Fig. 2 shows a comparison between the predicted ultimate horizontal load  $H_{ou-pred}$  according to Eq. 1 and the measured ultimate horizontal load  $H_{ou-meas}$  for 28 of the piles with measured pressuremeter limit pressures.

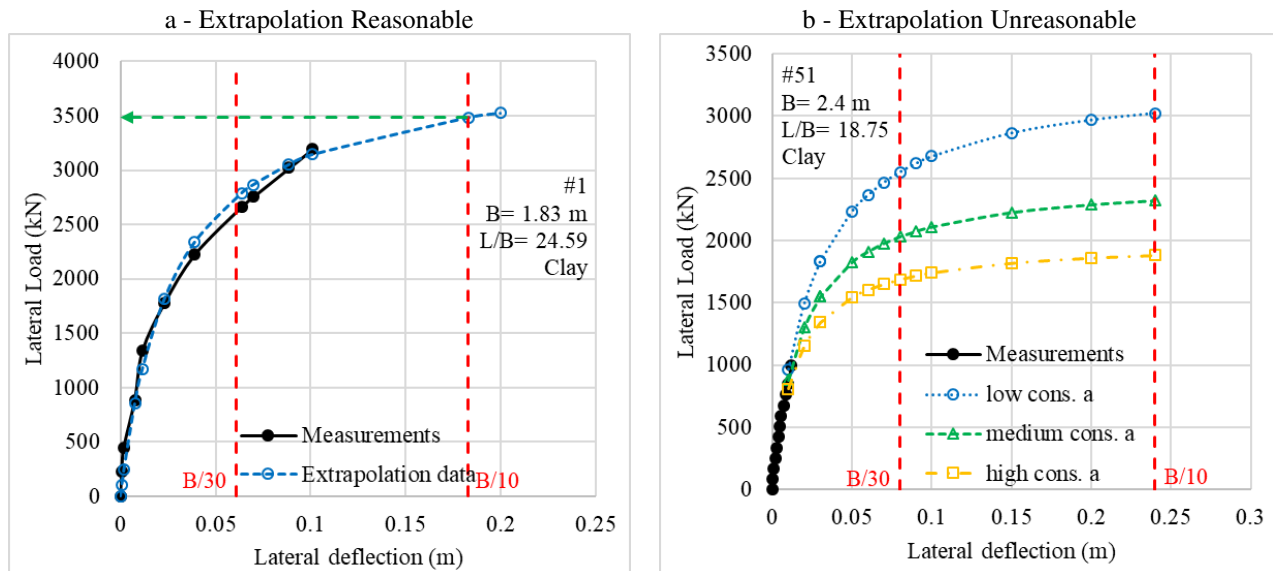


Figure 1. Extrapolation of the Load Displacement Curves.

Table 2. Extrapolation Cases for Ultimate Lateral Load Determination.

| Group                                 | No. | Criterion                   | Sand                |                        | Clay                |                        |
|---------------------------------------|-----|-----------------------------|---------------------|------------------------|---------------------|------------------------|
|                                       |     |                             | $B < 1.5 \text{ m}$ | $B \geq 1.5 \text{ m}$ | $B < 1.5 \text{ m}$ | $B \geq 1.5 \text{ m}$ |
| Extrapolation not needed              | 1.  | $y_{max} \geq B/10$         | 15                  | 7                      | 20                  | 2                      |
| Extrapolation needed and reasonable   | 2.  | $B/30 \leq y_{max} < B/10$  | 13                  | 5                      | 8                   | 4                      |
| Extrapolation needed but unreasonable | 3.  | $B/100 < y_{max} \leq B/30$ | 5                   | 6                      | 3                   | 5                      |
|                                       | 4.  | $y_{max} < B/100$           | 0                   | 12                     | 0                   | 5                      |
|                                       |     | total                       | 33                  | 30                     | 31                  | 16                     |

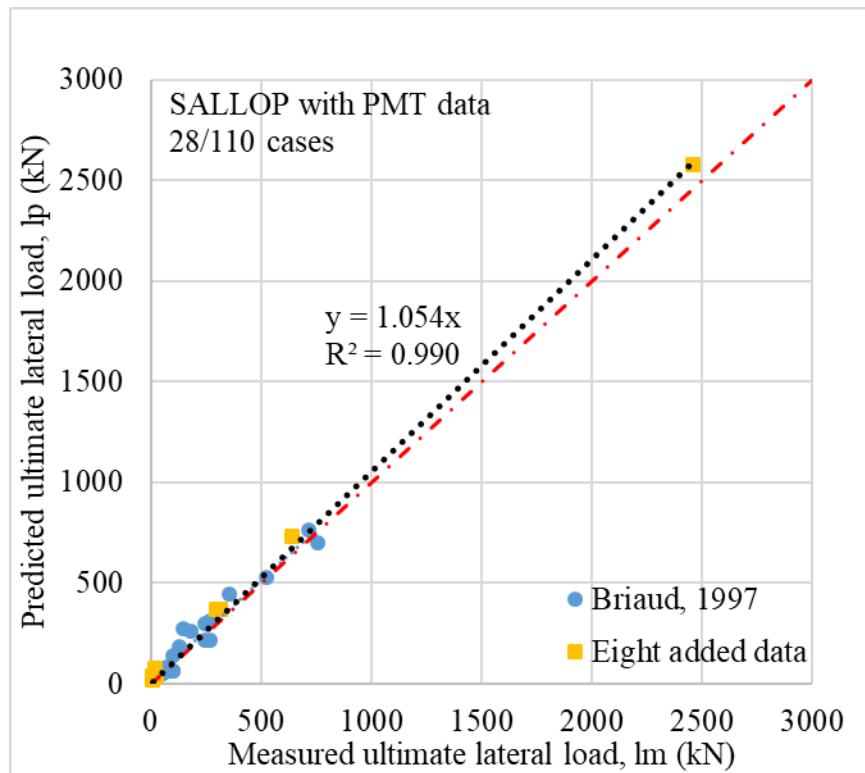


Figure 2. The SALLOP Predicted versus Measured Ultimate Load with PMT Data.

## QUANTITIES PREDICTED

Both displacements and loads were predicted. The predicted displacements were the lateral displacements  $y_o$  near the ground surface at various fractions of the ultimate load  $H_{ou}$ , defined as the load at a displacement equal to one tenth of the pile diameter or width ( $B/10$ ). These fractions were 10, 25, 33, and 50% of  $H_{ou}$ , as shown in Figure 2(a). In this figure, L is the pile length, LLT refers to the Lateral Load Test, and LPILE refers to the software used to make the predictions.

The predicted loads were the horizontal loads  $H_o$  applied near the ground surface at different values of the displacement  $y_o$  expressed as a fraction of the pile diameter or width. These fractions were 1, 2, 5, and 10% of the pile diameter or width B as shown in

Figure 2(b).

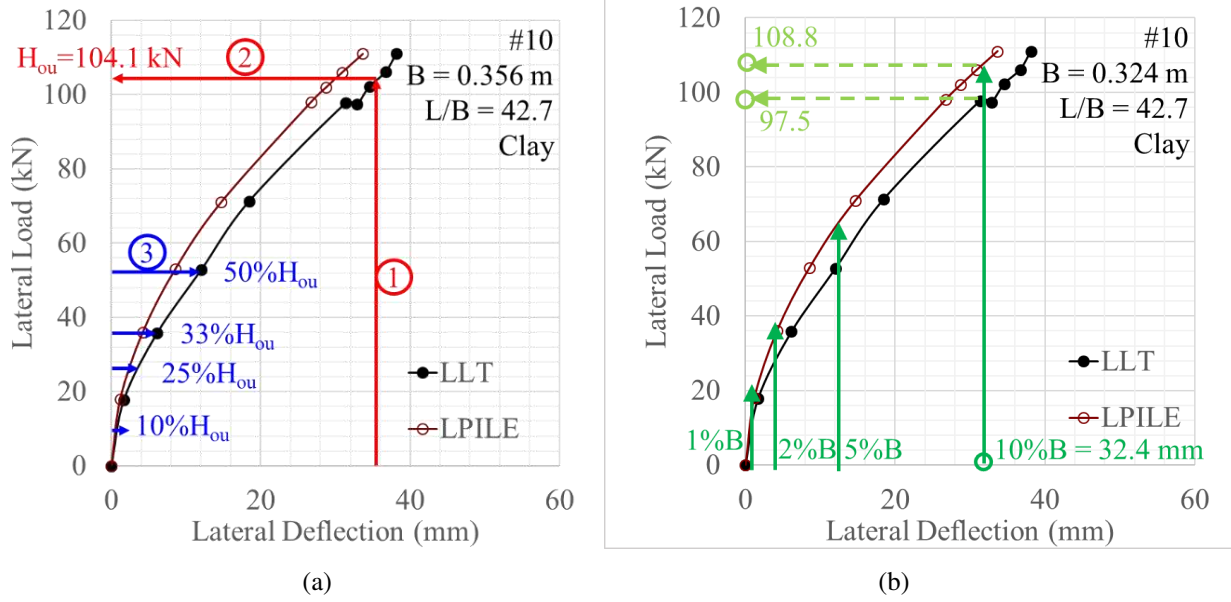


Figure 2. Predicted Quantities: (a) Displacements at Various Fractions of Ultimate Load, and (b) Load at Deflections Equal to Various Fractions of Pile Diameter.

### COMPARING THE PREDICTIONS WITH THE MEASUREMENTS

The predictions using the selected P-y curves and the program LPILE were performed for all 110 load tests (Briaud & Wang, 2018). Example results are shown in Figure 3 and Figure 4 for two small diameter piles and in Figure 5 and Figure 6 for two large diameter piles.

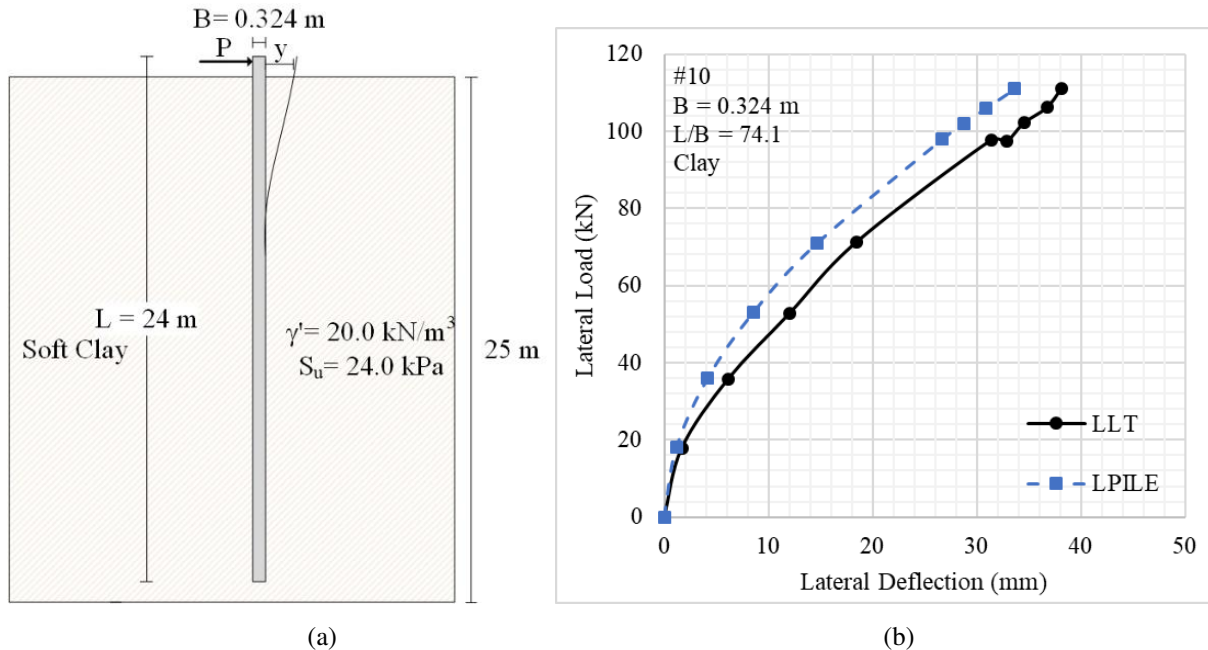


Figure 3. Case RN 10: (a) Soil Stratigraphy, (b) Comparison between Measured and Predicted Lateral Deflection Curve of Edmonton Test.

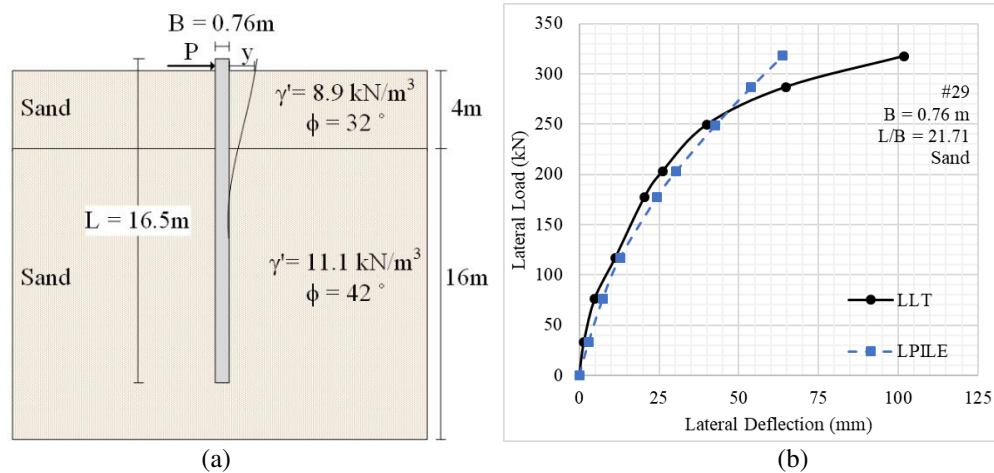


Figure 4. Case RN 29: (a) Soil Stratigraphy, (b) Comparison between Measured and Predicted Lateral Deflection Curve of Stuart Test.

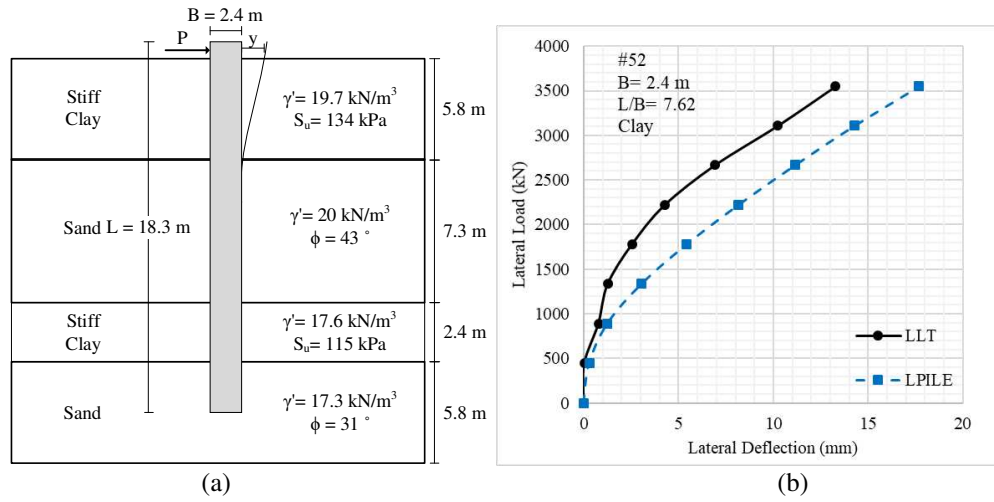


Figure 5. Case RN 52: (a) Soil Stratigraphy, (b) Comparison between Measured and Predicted Lateral Deflection Curve of Hawthorne Test.

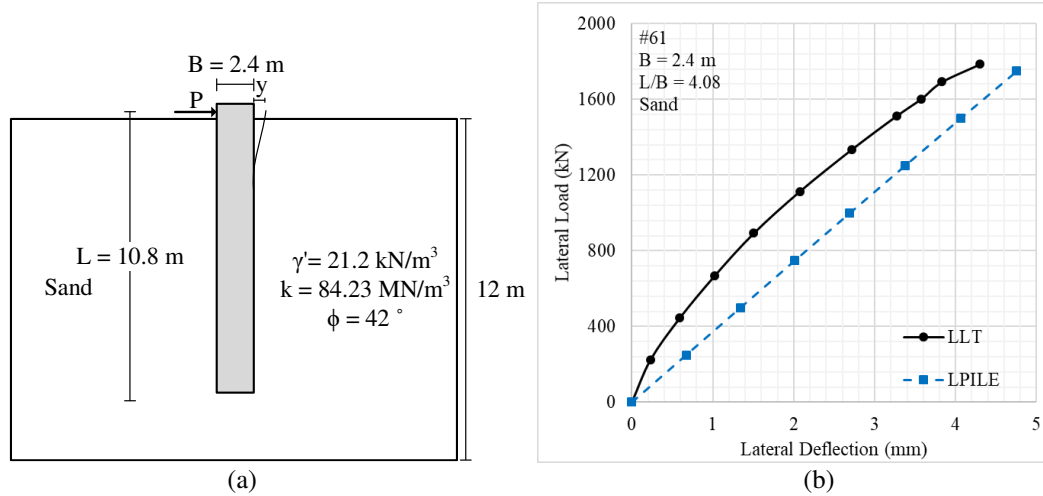


Figure 6. Case RN 62: (a) Soil Stratigraphy, (b) Comparison between Measured and Predicted Lateral Deflection Curve of Glenwood Canyon (West) Test.

First, the comparison is presented as the ratio of the predicted over measured load for a given deflection plotted against the pile diameter. The selected pile head deflections are 1, 2, 5, and 10% of the pile diameter. The comparison is done separately for the two types of soil (sand and clay). For the sand, the P-y curves of API Sand (2010) are selected. For the soft clays, the P-y curves of Matlock (1970) are chosen; for the stiff clays, the P-y curves of Reese et al. (1975) are used. For layered soils, the case is classified as sand or clay by selecting the dominant soil type within the top third of the embedded pile length.

Second, the comparison is presented as the ratio of the predicted over measured deflection for a given load plotted against the pile diameter. The selected lateral loads are equal to 10, 25, 33, and 50% of the ultimate lateral load. The ultimate load was taken as the load at a pile-head displacement corresponding to 0.1B, where B is the pile diameter (Briaud, 2013). The same distinction between soil types was used for loads and deflections.

### Comparison of Loads in Sand

Figure 7 shows the ratio of the predicted over measured load ( $L_p/L_m$ ) at lateral pile head displacements of 1, 2, 5, and 10% of the pile diameter as a function of pile diameter. The average predicted over measured load ratios are 0.791, 0.867, 0.908, and 0.954 in sand for the 1, 2, 5, and 10%, respectively; thus, the load corresponding to these deflections is underpredicted by about 12% on average. While the average ratio  $L_p/L_m$  indicates a good prediction on average, the scatter is quite large as the ratio  $L_p/L_m$  varies between 0.28 and 1.85. Note that the coefficient of variation decreases as the predicted deflection becomes larger. The trend lines in Fig. 8 indicate that there is a diameter effect for piles in sand and that the  $L_p/L_m$  ratio increases with diameter.

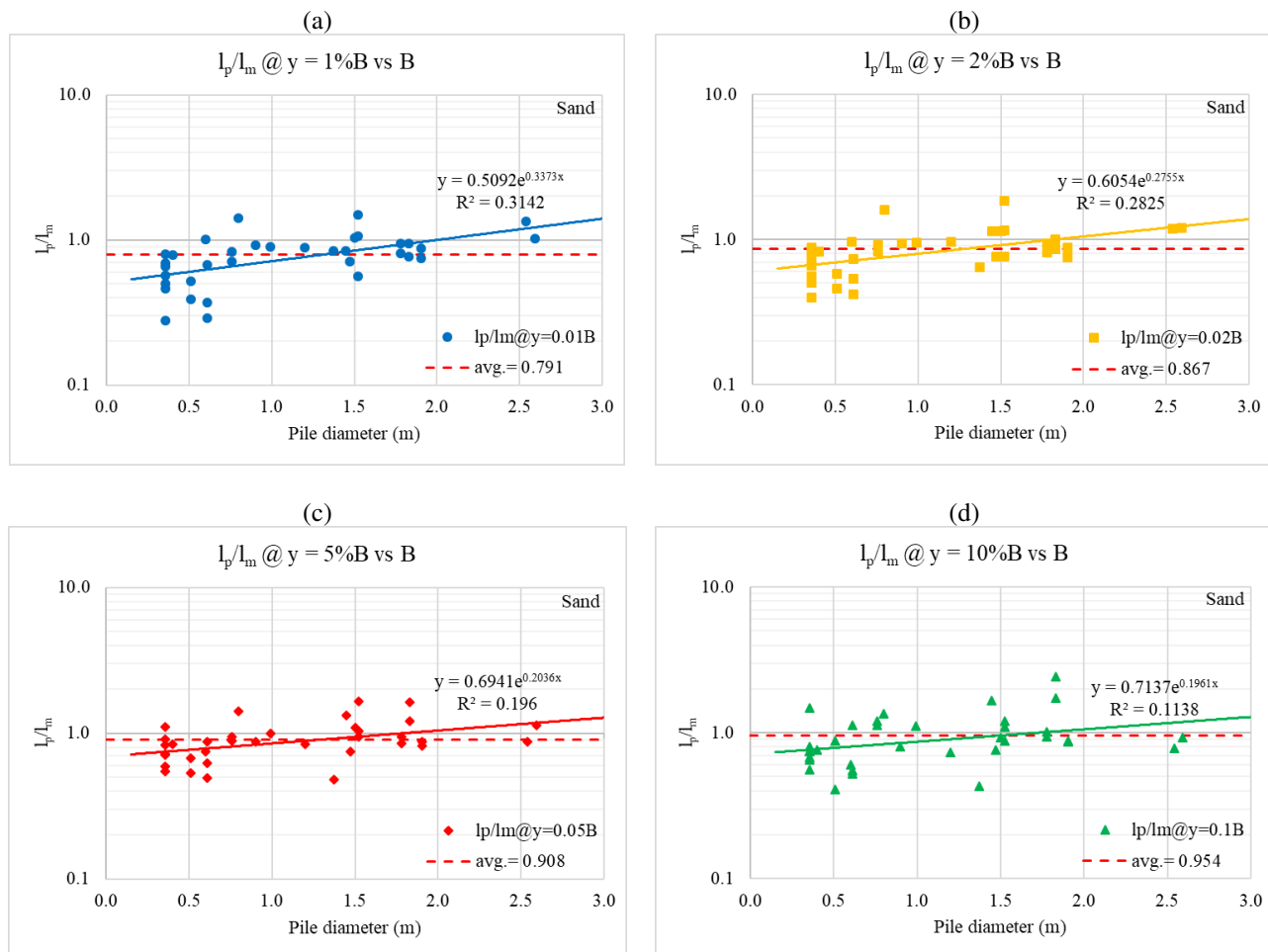


Figure 7. Ratio of Predicted over Measured Load versus Pile Diameter at Deflections Equal to (a) 1, (b) 2, (c) 5, and (d) 10 Percent of Pile Diameter for the No Extrapolation and Reasonable Extrapolation Data in Sand.

## Comparison of Loads in Clay

Figure 9 shows the ratio of the predicted over measured load ( $L_p/L_m$ ) at lateral pile head displacements of 1, 2, 5, and 10% as a function of the pile diameter. The average predicted over measured load ratio is equal to 1.009, 0.955, 0.919, and 1.009 in clay for the 1, 2, 5, and 10%, displacement, respectively. Therefore, the predicted over measured load ratio  $L_p/L_m$  is generally close to 1 and decreases with the pile diameter, approaching an extrapolated value of 0.3 to 0.4 for 3 m diameter piles. This decreasing trend of  $L_p/L_m$  with increasing diameter is the opposite of the trend observed for piles in sand. The scatter is quite large and the ratio  $L_p/L_m$ , varies between 0.32 and 2.67.

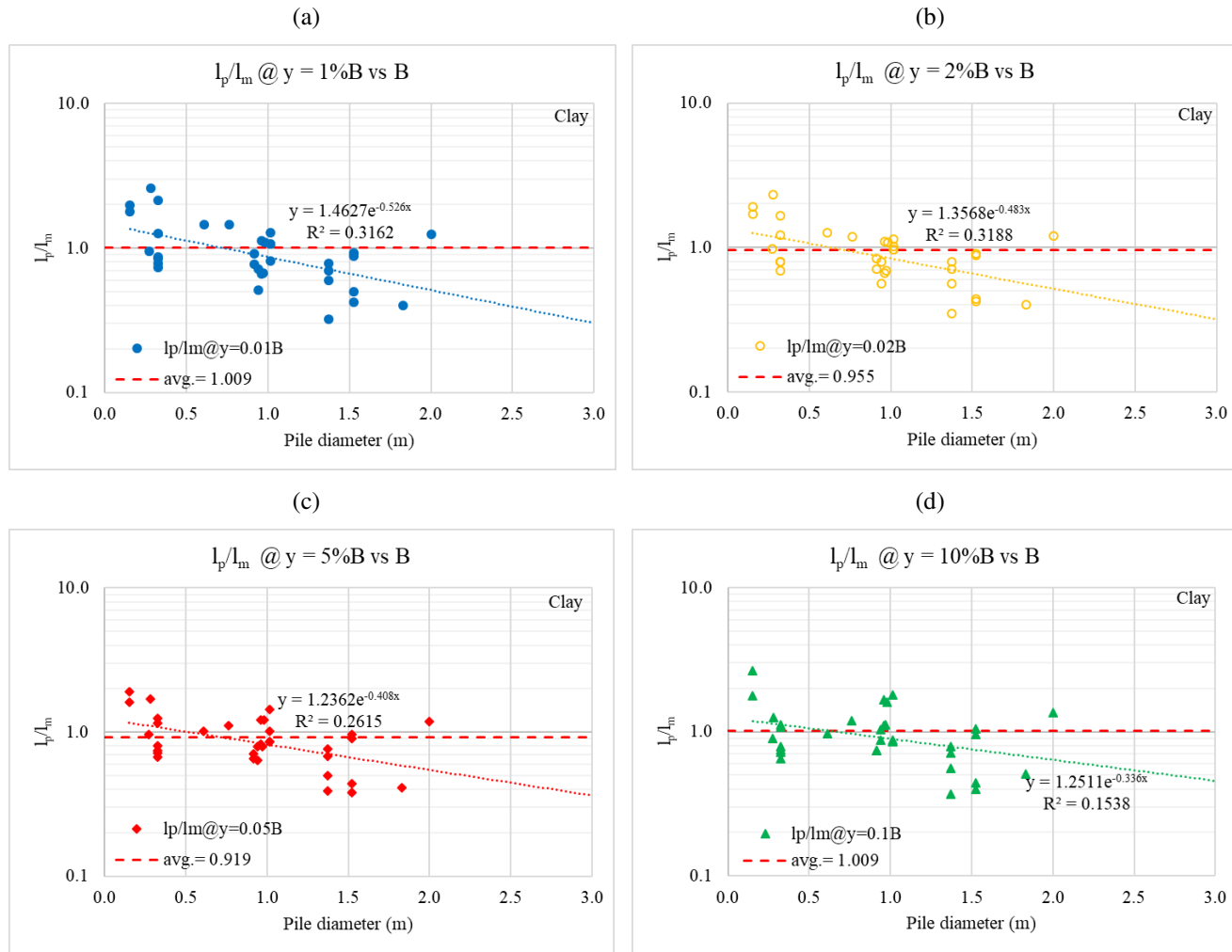


Figure 9. Ratio of Predicted over Measured Load versus Pile Diameter at Deflections Equal to (a) 1, (b) 2, (c) 5, and (d) 10 Percent of Pile Diameter with No Extrapolation and Reasonable Extrapolation Data in Clay.

## Comparison of deflections in sand

The two previous sections presented the comparison of predicted and measured loads for given deflections varying from 1 to 10% of the diameter  $B$ . This section presents the comparisons of predicted and measured deflections at given percentages of the ultimate load  $H_{ou}$ . These percentages were set at 10, 25, 33, and 50% of the ultimate lateral load  $H_{ou}$ . The ultimate load was taken as the load corresponding to a pile-head lateral displacement of  $0.1B$ , where  $B$  is the pile diameter (Briaud, 2013). As explained previously, since it was not possible to get a reasonable estimate of the ultimate load in all cases, the database used for comparing predicted and measured deflection consisted of 69 cases with 35 in sand.

The measured deflections were compared to the predicted deflections using LPILE and the P-y curves. Fig. 10 shows the ratio of the predicted deflection  $y_p$  over the measured deflection  $y_m$  as a function of the pile diameter. The average ratios  $y_p/y_m$  are 2.173, 1.730, 1.630, and 1.464 for 10, 25, 33, and 50% of the ultimate load, respectively. Thus, the data show that the predicted deflections are typically significantly overpredicted for small diameter piles but that the predicted deflections get closer to the measured deflections for larger diameter piles, indicating a decreasing trend in  $y_p/y_m$  as  $B$  increases. Overall, the ratio  $y_p/y_m$  ranged between 0.29 and 6.02 for piles in sand.

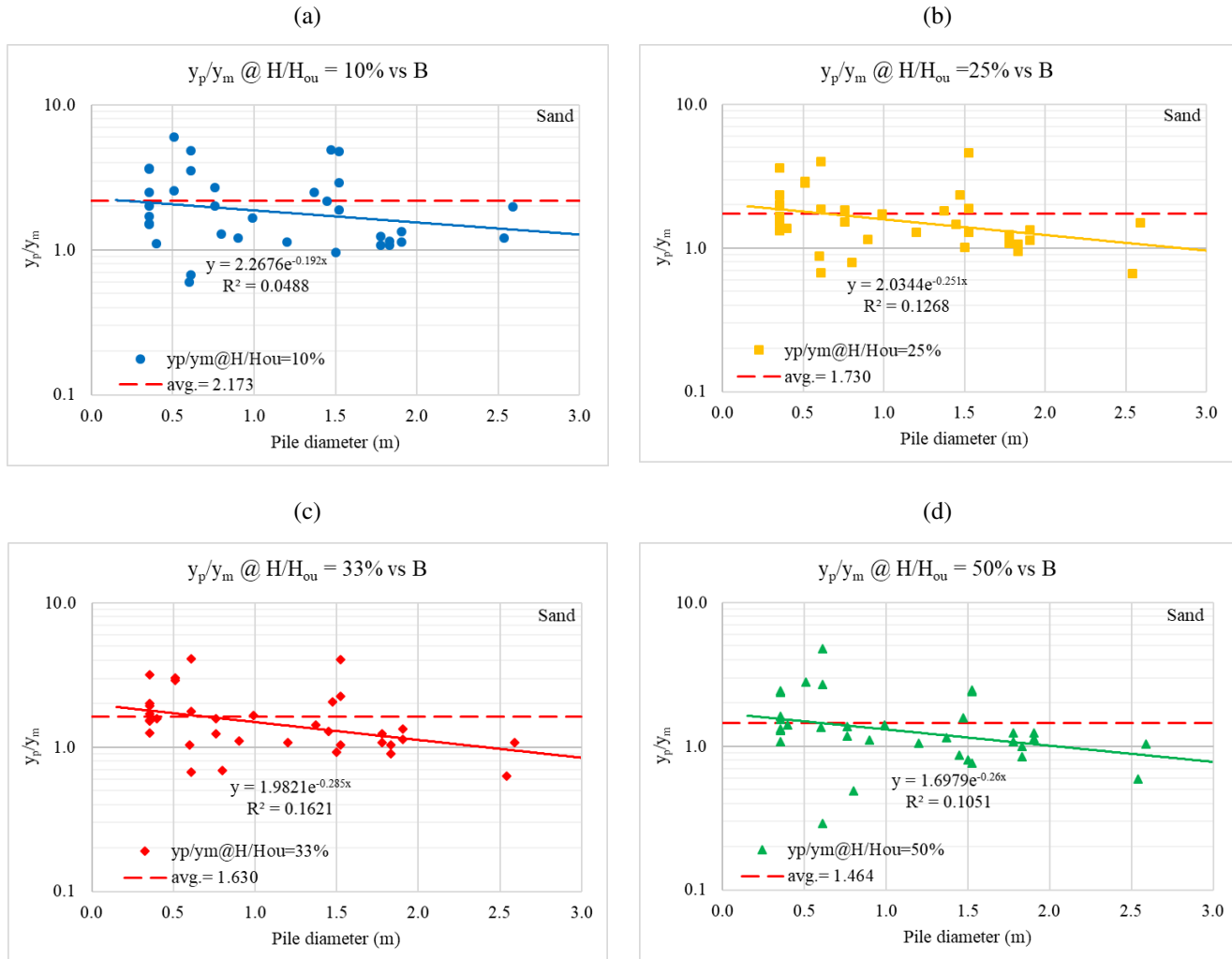


Figure 10. Ratio of Predicted and Measured Deflection versus Pile Diameter at Applied Loads Equal to (a) 10, (b) 25, (c) 33, and (d) 50 Percent of the Ultimate Lateral Load with No Extrapolation and Reasonable Extrapolation Data in Sand.

### Comparison of Deflections in Clay

This section presents the comparison between predicted and measured deflections in clay at given percentages of the ultimate load  $H_{ou}$  taken as the load corresponding to a pile-head lateral displacement of  $0.1B$ , where  $B$  is the pile diameter (Briaud, 2013). The measured deflections were obtained at 10, 25, 33, and 50% of the ultimate lateral load  $H_{ou}$ . These measured deflections were then compared to the predicted deflections using LPILE. Fig. 11 shows the ratio of the predicted deflection  $y_p$  over the measured deflection  $y_m$  as a function of the pile diameter for the 34 piles in clay for which a reasonable estimate of the ultimate load could be obtained. The average of the ratio  $y_p/y_m$  is 1.702, 2.169, 2.721, and 4.391 for the 10, 25, 33, and 50% of the ultimate load, respectively. As can be seen, the deflections are overpredicted on average and more so for the larger pile diameters. This increase in  $y_p/y_m$  with  $B$  in clay is contrary to the trend in sand. The deflections of smaller piles are

predicted with less conservatism; for larger diameter piles, however, the deflections are significantly overpredicted. Overall, the ratio  $y_p/y_m$  ranged between 0.09 and 45.13 for piles in clay.

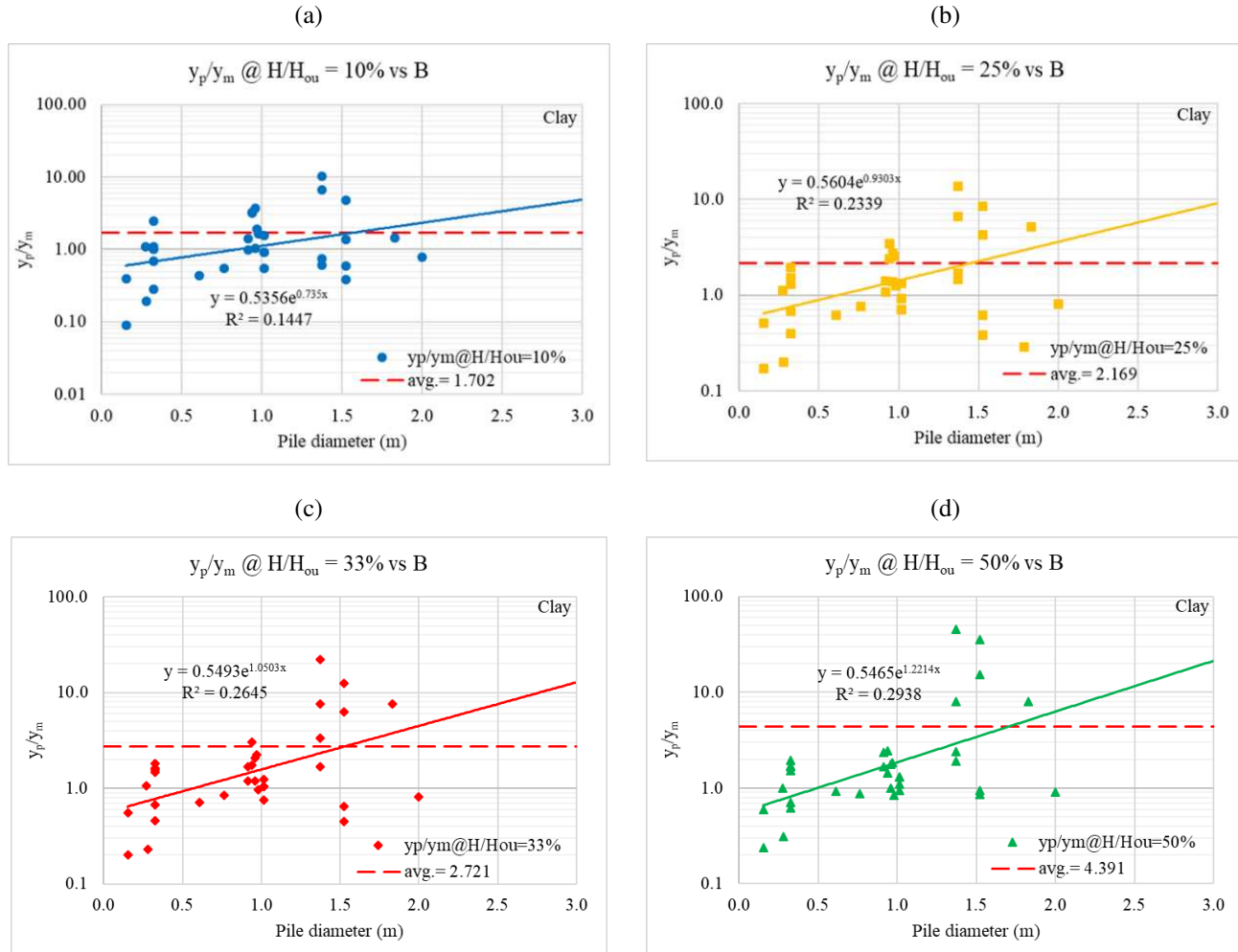
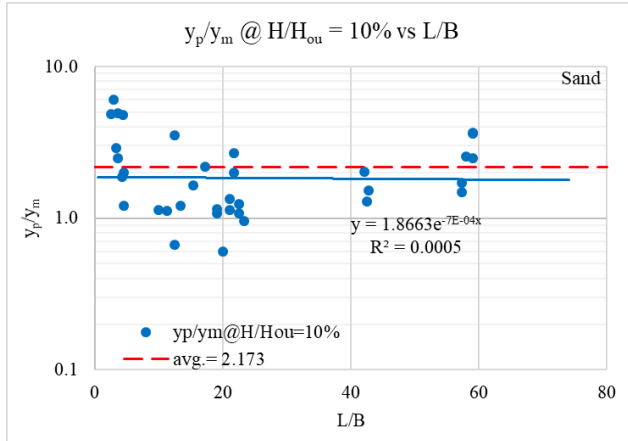


Figure 11. Ratio of Predicted and Measured Deflection versus Pile Diameter at Applied Loads Equal to (a) 10, (b) 25, (c) 33, and (d) 50 Percent of the Ultimate Lateral Load with No Extrapolation and Reasonable Extrapolation Data in Clay.

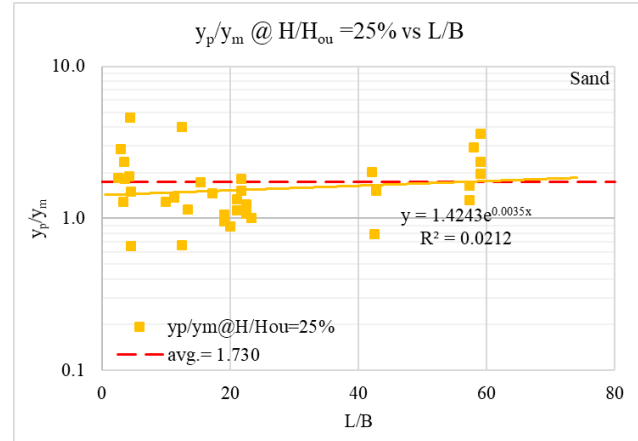
#### Pile Length to Diameter Ratio (L/B) Effect on the Comparison of Deflections in both Sand and Clay

To evaluate the influence of the length to diameter ratio (L/B) on the predictions, the predicted over measured deflection ratio ( $y_p/y_m$ ) is plotted against the L/B ratio in Fig. 12 for sand and in Fig. 13 for clay. Evidently, there is no discernable influence of L/B on  $y_p/y_m$  except at lower values of L/B, particularly in clay. This tends to indicate that, for L/B ratios less than about 5, the contributions of the base shear, the base moment, and the side shear resistances to overturning become significant and should be accounted for (Wang et al., 2022).

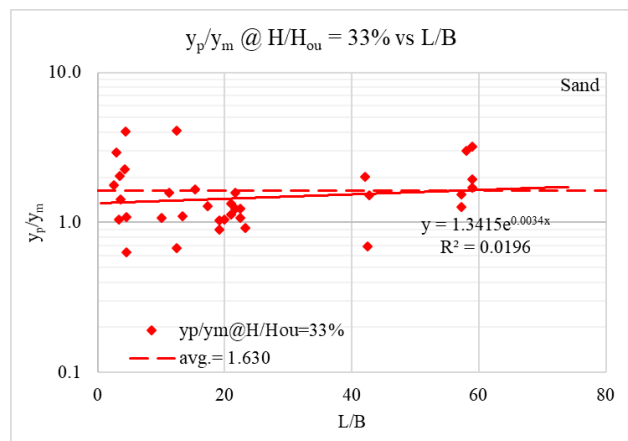
(a)



(b)



(c)



(d)

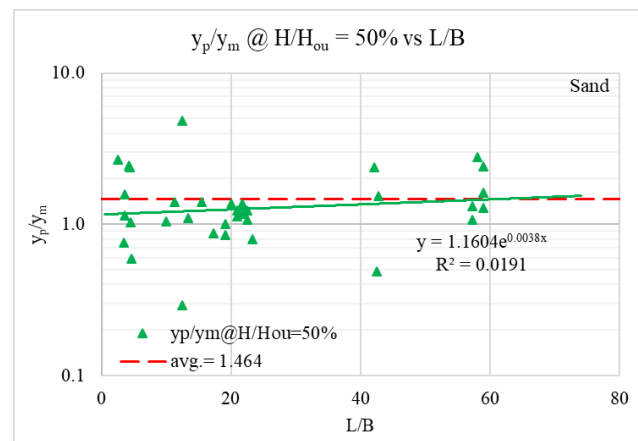
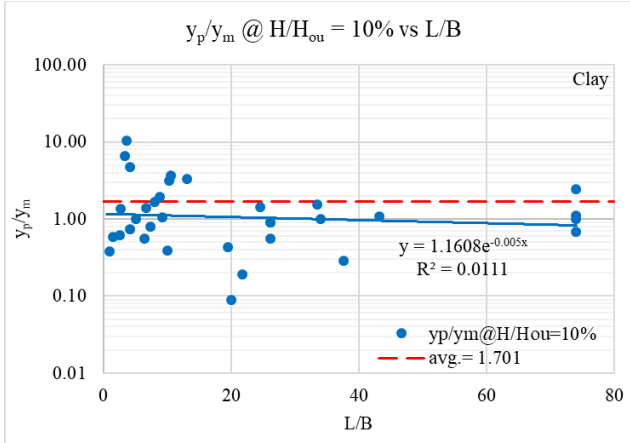
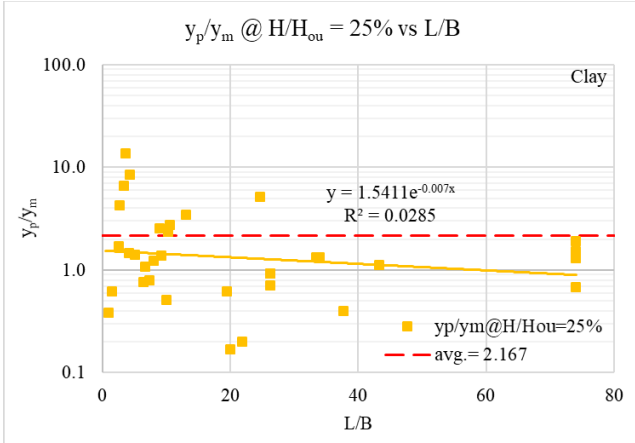


Figure 12. Ratio of Predicted Over Measured Deflection versus Pile Length over Diameter at Applied Loads Equal to (a) 10, (b) 25, (c) 33, and (d) 50 Percent of the Ultimate Lateral Load in Sand.

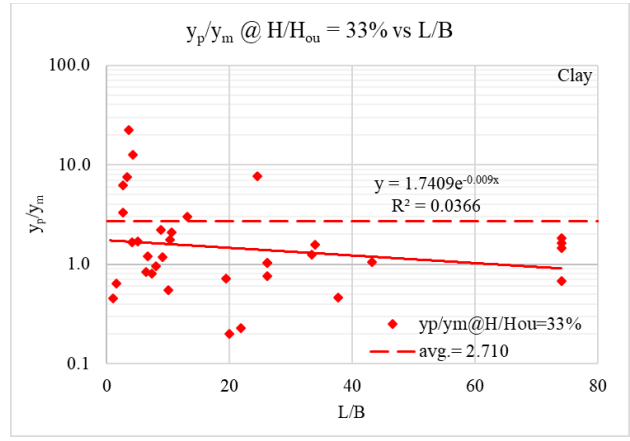
(a)



(b)



(c)



(d)

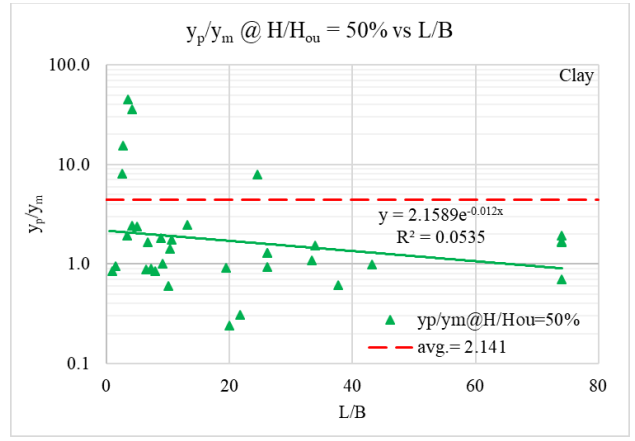


Figure 13. Ratio of Predicted over Measured Deflection versus Pile Length over Diameter at Applied Loads Equal to (a) 10, (b) 25, (c) 33, and (d) 50 Percent of the Ultimate Lateral Load in Clay.

#### Pile Installation Effect on the Comparison of Deflections in both Sand and Clay

Piles can be bored or driven into the ground. The influence of this distinction is studied in this section by plotting separately, for bored piles and driven piles in sand and in clay, the ratio of predicted over measured deflection ( $y_p/y_m$ ) versus pile diameter (B) at applied loads equal to 10, 25, 33, and 50 percent of the ultimate lateral load. Fig. 14 shows no significant difference between bored and driven piles in sand. A larger difference is observed in clay (Fig. 15); indeed, the regression lines are quite different for both pile types. It is important to note that the biggest diameter in the database for driven piles in clay is 1 m; thus, the extrapolation to 3 m is very doubtful. The comparison for piles in clay with diameters up to 1 m does not show any significant difference between bored and driven piles. Overall, the difference between bored and driven piles does not seem to have a significant influence on the precision of the predictions.

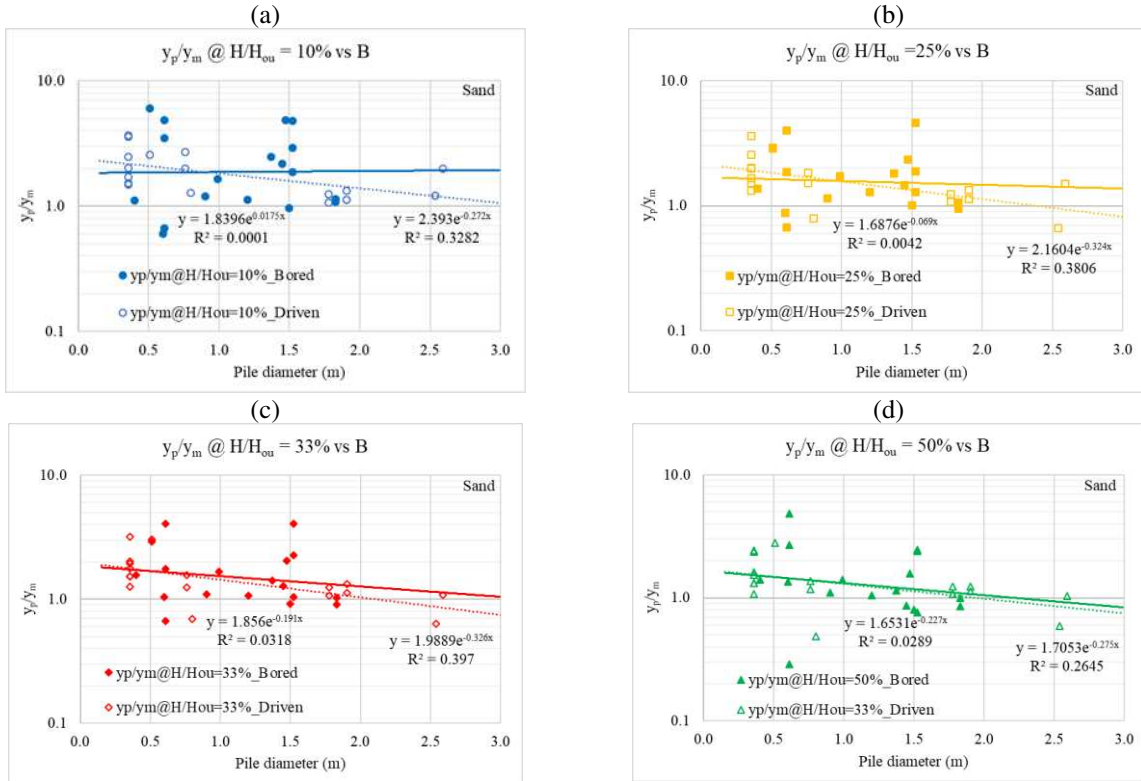


Figure 14. Ratio of Predicted over Measured Deflection versus Pile Diameter at Applied Loads Equal to (a) 10, (b) 25, (c) 33, and (d) 50 Percent of the Ultimate Lateral Load between Bored and Driven Piles in Sand.

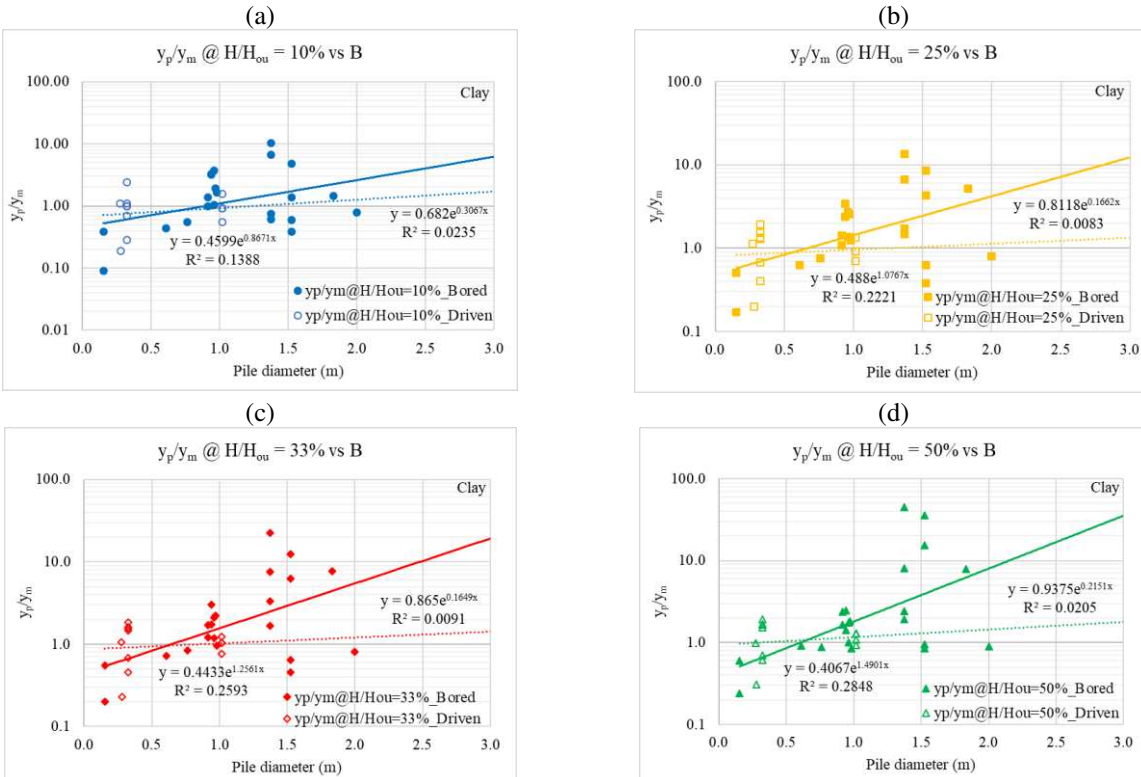


Figure 15. Ratio of Predicted over Measured Deflection versus Pile Diameter at Applied Loads Equal to (a) 10, (b) 25, (c) 33, and (d) 50 Percent of the Ultimate Lateral Load between Bored and Driven Piles in Clay.



---

## PROPOSED P-Y CURVES MODIFICATIONS TO MINIMIZE THE EFFECT OF B

The previous sections indicated that when using the P-y criteria developed by API (2010), Matlock (1970), and Reese et al. (1974), the following conclusions are reached:

1. In sand, on average the loads are slightly underpredicted and the  $L_p/L_m$  ratio increases with pile diameter B.
2. In sand, on average the deflections are significantly overpredicted and the  $y_p/y_m$  ratio decreases with pile diameter B.
3. In clay, on average the loads are close to the measurements and the  $L_p/L_m$  ratio decreases with pile diameter B.
4. In clay, on average the deflections are significantly overpredicted and the  $y_p/y_m$  ratio increases with pile diameter B.

The following sections describe an attempt at correcting those trends by modifying the P-y curves.

### P-y Curves Modification in Sand

The API Sand Model (2010) was selected for this study because it is widely used in practice. This model was developed based on the recommendations from Reese et al. (1974) and then O'Neill and Murchison (1983). It uses the modulus of subgrade reaction  $k$  defined as the ratio of the mean lateral pressure  $p$  on the pile (line load divided by width) at a depth  $z$  divided by the displacement  $y$  at that depth.

$$k = \frac{p}{y} \quad (2)$$

The parameter  $k$  is in units of  $\text{kN}/\text{m}^3$ . The elastic formula for the displacement of a loaded area is given by:

$$y = I(1 - \nu^2) \times \frac{pB}{E} \quad (3)$$

Where  $y$  is the displacement,  $I$  is primarily a shape factor,  $\nu$  is Poisson's ratio,  $p$  is the average pressure on the area,  $B$  is the width of the loaded area, and  $E$  is the soil modulus. Using Eq. 2 and 3 above gives  $k$  as:

$$k = \frac{p}{y} = \frac{E}{I(1 - \nu^2)B} \quad (4)$$

This indicates that the modulus of subgrade reaction  $k$  increases with the soil modulus  $E$  and decreases with the pile diameter  $B$ . Thus,  $k$  values developed on the basis of small diameter pile load tests cannot be directly used for much larger diameter piles. This is the basis for the proposed modification. Eq. 4 further indicates that the  $k$  values obtained from small diameter pile load tests will be higher (stiffer response) than the  $k$  values associated with much larger diameter piles. As such, the use of  $k$  values derived from pile load tests on small diameter piles will lead to underestimated deflections for a given load and overestimated loads for a given displacement when predicting the behavior of large diameter piles. This is what was observed in the database as shown earlier. It was also observed that in sand the deflections were significantly overestimated on average and therefore the  $k$  value needed to be generally increased.

To accomplish the improvement, the  $k$  values were multiplied by a modification factor  $n_k$  which would be larger than 1 but decrease with  $B$ . Various values of this  $n_k$  factor were used for each pile load test until the ratio of predicted deflection over measured deflection  $y_p/y_m$  for the load at 33% of ultimate was optimized (closest to 1). The dots in Fig. 16 represent the optimum values of  $n_k$  for 35 load tests including the 22 cases where no extrapolation was necessary and the 13 cases where extrapolation was necessary and considered reasonable. Based on these results (dots in Fig. 16) and on the observation that the modification should aim at increasing the average values of  $k$  while creating a decreasing trend in  $k$  as the pile diameter increases, the following function for  $n_k$  was proposed (dash line in Fig. 16):

$$k_{\text{mod}} = n_k k \quad \text{with} \quad n_k = 3 \text{ when } B \leq 1.0 \text{ m} \\ \text{and} \quad n_k = 3/B \text{ when } B > 1.0 \text{ m} \quad (5)$$

The ratio  $y_p/y_m$  vs.  $B$  before and after applying the  $n_k$  correction factor is shown in Fig. 17. The figure indicates that the average ratio  $y_p/y_m$  at 33% of ultimate load drops from 1.630 to 1.168, that the range of the ratio of  $y_p/y_m$  narrows from 0.29 to 6.02 to 0.28 to 3.80, and that the  $R^2$  decreases from 0.1621 to 0.0322. Note that the lower  $R^2$  indicates that the  $y_p/y_m$  ratio becomes more independent of  $B$ , which is the goal of this proposed modification.

The correction factor  $n_k$  was developed by optimizing the comparison between the  $y_p/y_m$  ratio for deflections at 33% of ultimate load. The proposed  $n_k$  values were then checked against the other deflection levels including 10, 25, and 50% of ultimate load by generating figures similar to those of Fig. 17 for the other load levels. These are shown in Fig. 18. Overall, the predicted deflections are still somewhat larger than the measured values on average, but the dependency on the pile diameter is significantly decreased as indicated by the very low  $R^2$ .

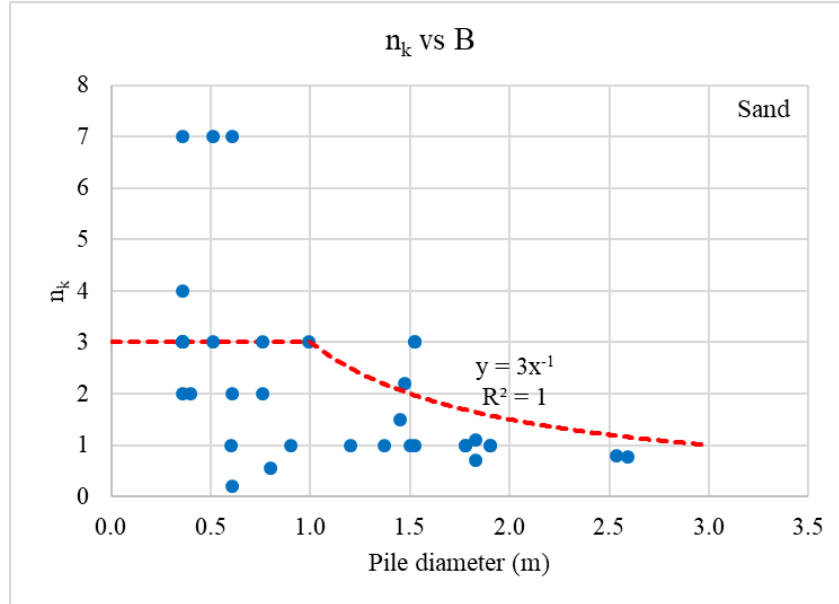


Figure 16. Correction Coefficient for the Subgrade Modulus ( $n_k$ ) versus Pile Diameter and Proposed Curve.

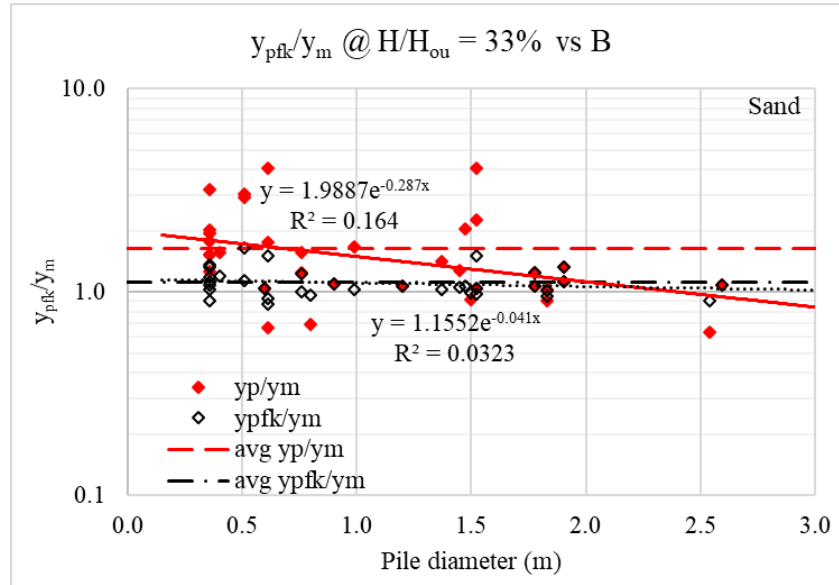


Figure 17. Ratio of Predicted over Measured Deflection versus Pile Diameter at Applied Loads Equal to 33% of the Ultimate Lateral Load Before and After Applying the Proposed Modification in Sand.

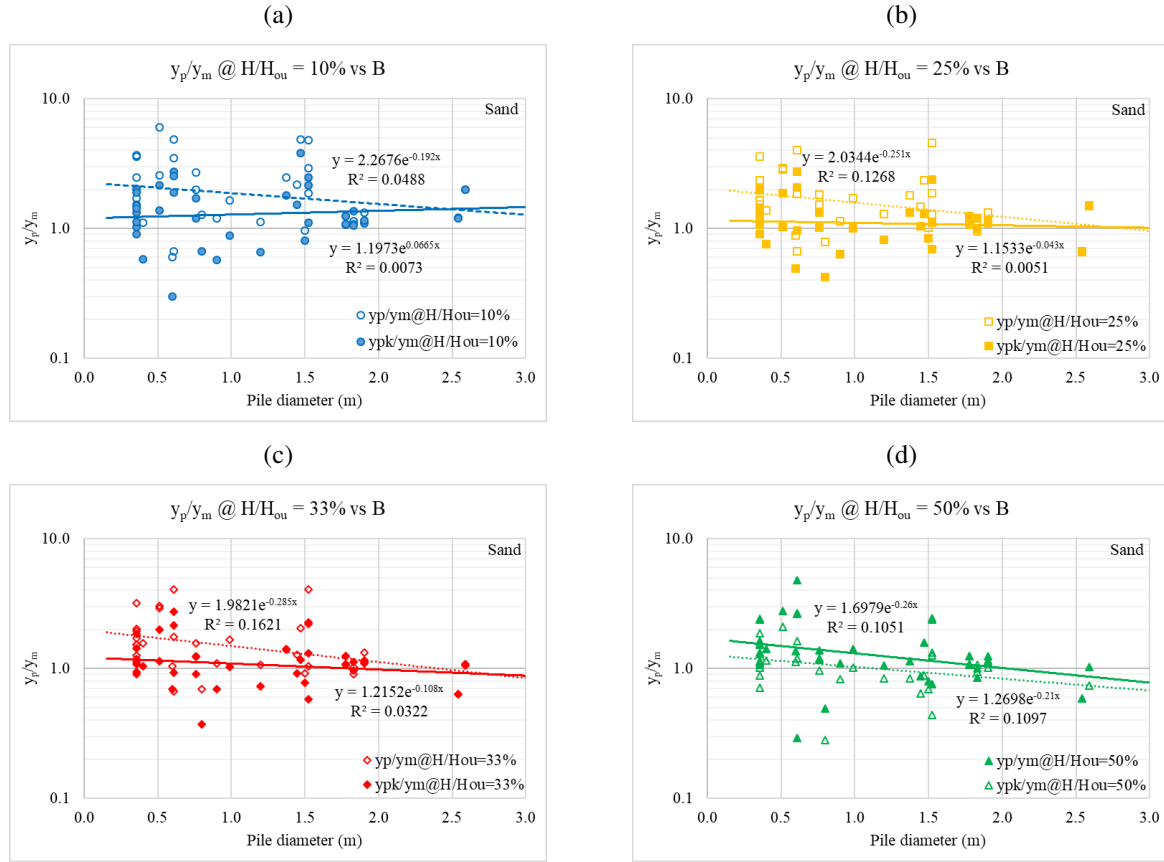


Figure 18. Ratio of Predicted over Measured Deflection versus Pile Diameter at Applied Loads Equal to (a) 10, (b) 25, (c) 33, and (d) 50 Percent of the Ultimate Lateral Load Before and After the Proposed Modification in Sand. In the Legend,  $y_p$  is the Predicted Deflection Before Correction and  $y_{pk}$  is the Predicted Deflection After Correction.

### P-y Curves Modification in Clay

The soft and stiff clay P-y models (Matlock, 1970 and Reese et al., 1975) were selected for this study as they are used commonly in practice. In both criteria, the stiffness of the P-y curve is controlled by the deflection  $y_{50}$  at one-half the ultimate soil resistance;  $y_{50}$  is computed as follows:

$$y_{50} = 2.5 \times \epsilon_{50} \times B \quad (6)$$

Where  $B$  is the pile diameter and  $\epsilon_{50}$  is the vertical strain at one-half the maximum deviatoric stress in a triaxial test. The recommendations for selecting the strain  $\epsilon_{50}$  are tied to the undrained shear strength, and  $\epsilon_{50}$  varies between 0.005 for stiff clay and 0.02 for soft clay. In most cases in the clay database, an average value of the undrained shear strength was entered and thus a single value of  $\epsilon_{50}$  was used. This implies that the soil modulus was constant with depth. However, in most cases the soil modulus increased with depth mostly due to the increase in effective stress level. As shown next, this difference between an assumed constant modulus with depth and a true modulus increasing with depth can explain the trend of increasing predicted deflection with increasing diameter, as observed in the data.

A series of Finite Element Method (FEM) simulations were performed using Abaqus to evaluate the influence of the modulus profile on the predicted deflection. An elastic model was used to predict the behavior of the pile. The elastic part of the soil model was governed by the long-term modulus of the soil at each depth; this modulus was obtained as  $250 s_u$ , where  $s_u$  was the undrained shear strength of the soil. The Mohr-Coulomb Model was used to simulate the plastic behavior of the soil. The equation used for the soil modulus profile was:

$$\frac{E_m}{E_0} = 1 + mz \quad (7)$$

Where  $E_m$  is the modulus at a depth  $z$ ,  $E_0$  is the modulus at  $z = 0$ ,  $z$  is the depth in meters, and  $m$  is the slope of the profile in units of  $m^{-1}$ . If  $m = 0$ , the modulus is constant with depth; if  $m = 1$ , the modulus increases linearly with  $z$ . The modulus vs. depth profile in the FEM was represented by an increasing step function with each 1 m thick layer having a constant soil modulus given by Eq. 7. The soil model included a no tension condition and a limit on the friction at the interface between the pile and the soil. This limit was set at 0.4 times the normal stress on the pile surface.

Two piles were simulated, a 0.5 m diameter 10 m long pile and a 3 m diameter 10 m long pile. The pile modulus  $E_p$  and the soil modulus  $E_0$  at  $z = 0$  were kept constant, and 3 cases of soil modulus profiles were considered:  $m = 0$ ,  $m = 0.5$ , and  $m = 1$ . The diameter of the soil mesh was 10 times the diameter of the pile, and the depth of the soil mesh was 1.5 times the length of the pile (or 15 m). The soil and pile properties used in the FEM simulations can be found in Table 3 and 4, respectively. The load deflection curves obtained from the FEM simulations are shown in Fig. 19 for the 0.5 m diameter pile and in Fig. 20 for the 3 m diameter pile.

Table 3. Soil Properties Used in FEM Simulations.

| Soil | Unit weight $\gamma$ (kN/m <sup>3</sup> ) | Undrained shear strength $S_u$ (kPa) | Young's modulus $E$ (kPa) | Poisson's ratio $\nu$ | Cohesion $c$ (kPa) | Friction angle $\phi$ (°) |
|------|---|--------------------------------------|---------------------------|-----------------------|--------------------|---------------------------|
| Clay | 18  | 24                                   | $E_0=250S_u$              | 0.35                  | 50                 | 35                        |

Table 4. Pile Properties Used in FEM Simulations.

| Pile No. | Unit weight $\gamma_c$ (kN/m <sup>3</sup> ) | Pile diameter $B$ (m) | Pile length $L$ (m) | Aspect Ratio (L/B) | Young's modulus $E$ (kPa) | Poisson's ratio $\nu$ |
|----------|---|-----------------------|---------------------|--------------------|---------------------------|-----------------------|
| 1        | 24  | 0.5                   | 10                  | 20                 | 2E+07                     | 0.17                  |
| 2        |   | 3.0                   | 10                  | 3.33               |                           |                       |

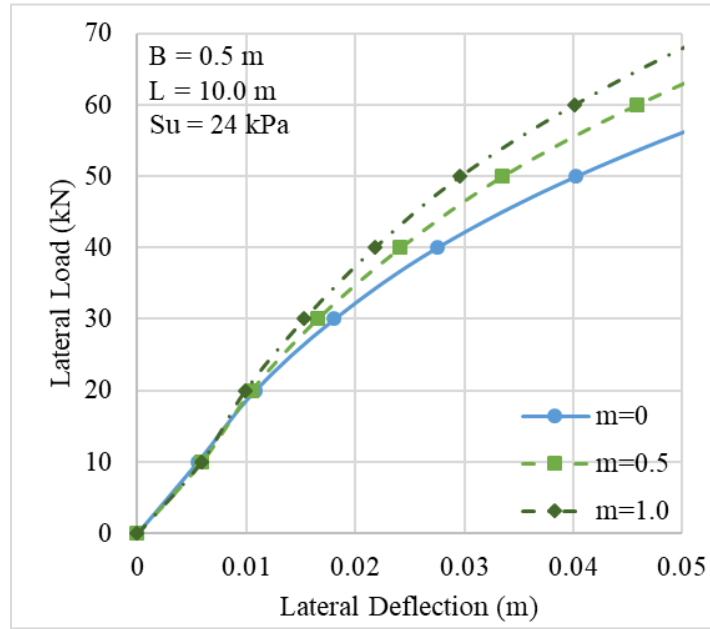


Figure 19. Load-Deflection Curves for Different Soil Modulus Profiles for the 0.5 m Diameter Pile in Abaqus.

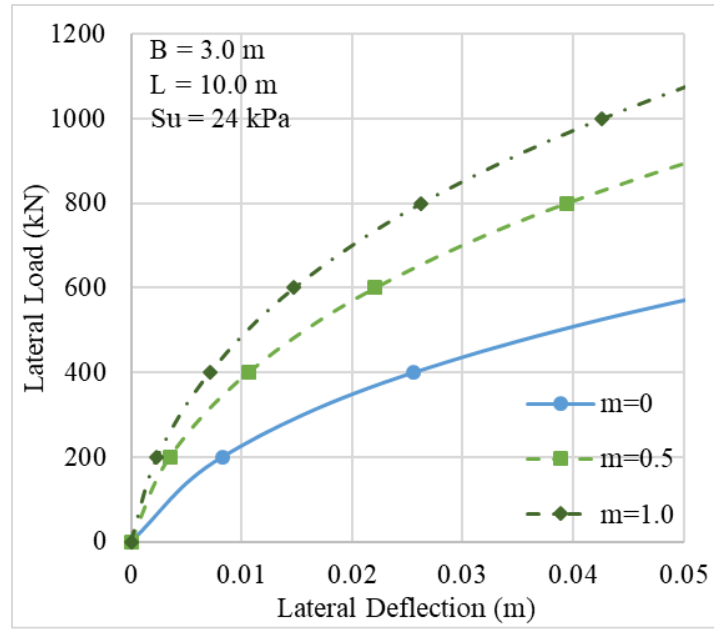


Figure 20. Load-Deflection Curves for Different Soil Modulus Profiles for the 3 m Diameter Pile in Abaqus.

If the predicted deflection for the 0.5 m diameter pile for  $m = 0$  is called  $y_{p-0.5-m=0}$ , the ratio  $y_{p-0.5-m=0}/y_{p-0.5-m=1}$  averages about 1.35 while the ratio  $y_{p-3.0-m=0}/y_{p-3.0-m=1}$  averages 3.5. In other words, the increase in soil modulus vs. depth has a much larger effect on the deflection of the large diameter pile than the deflection of the small diameter pile. Since this effect is not captured in the constant  $\epsilon_{50}$  approach, the deflections will generally be overestimated (1.35 and 3.5 are both larger than 1) and the overestimation will increase with the diameter (1.35 to 3.5). This is consistent with the data trends observed in the database and led to the following modification.

To maintain the current approach of using an equation to predict  $y_{50}$ , the equation itself was modified to be:

$$\frac{y_{50}}{B_o} = 1.8 \epsilon_{50} \left( \frac{B}{B_o} \right)^{0.3} \quad (8)$$

Where  $y_{50}$ ,  $B$ , and  $B_o$  must be in consistent units, and  $B_o$  is a reference width equal to 1 m. Stevens and Audibert (1979) had worked with a database of lateral load tests with pile diameters up to 1.5 m. They observed a similar trend of increase in overprediction with an increase in pile diameter. They proposed at the time to modify  $y_{50}$  according to the following equation which was non-dimensionalized by the authors.

$$\frac{y_{50}}{B_o} = 1.4 \epsilon_{50} \left( \frac{B}{B_o} \right)^{0.5} \quad (9)$$

The TAMU-Lateral database extends the data to piles up to 2.8 m in diameter and proposes an explanation for the observed trend. Eq. 8 leads to a correction factor for  $y_{50}$  given by:

$$y_{50\text{mod}} = n_y y_{50} \text{ with } n_y = 0.72 \left( \frac{B}{B_o} \right)^{-0.7} \quad (10)$$

Fig. 21 shows the correction factor  $n_y$  as a function of the pile width  $B$ . The proposed  $n_y$  values were checked against the deflection levels at 10, 25, 33, and 50% of ultimate load by generating figures similar to those in Fig.11. The results are shown in Fig. 22, indicating a significant improvement.

Overall, the predicted deflections are still somewhat larger than the measured values on average, but the dependency on the pile diameter is significantly decreased as indicated by the very low  $R^2$ .

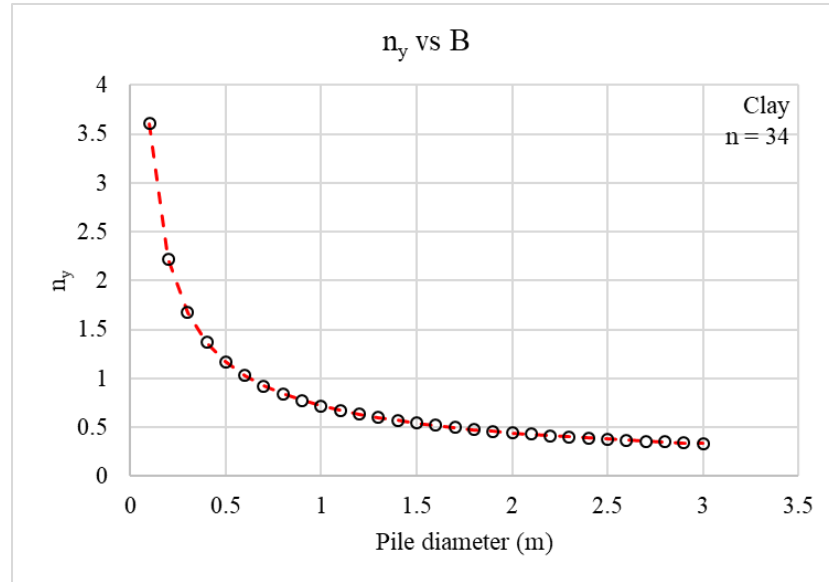


Figure 21. Correction Coefficient for the  $y_{50}$  ( $n_y$ ) versus Pile Diameter and Proposed Curve.

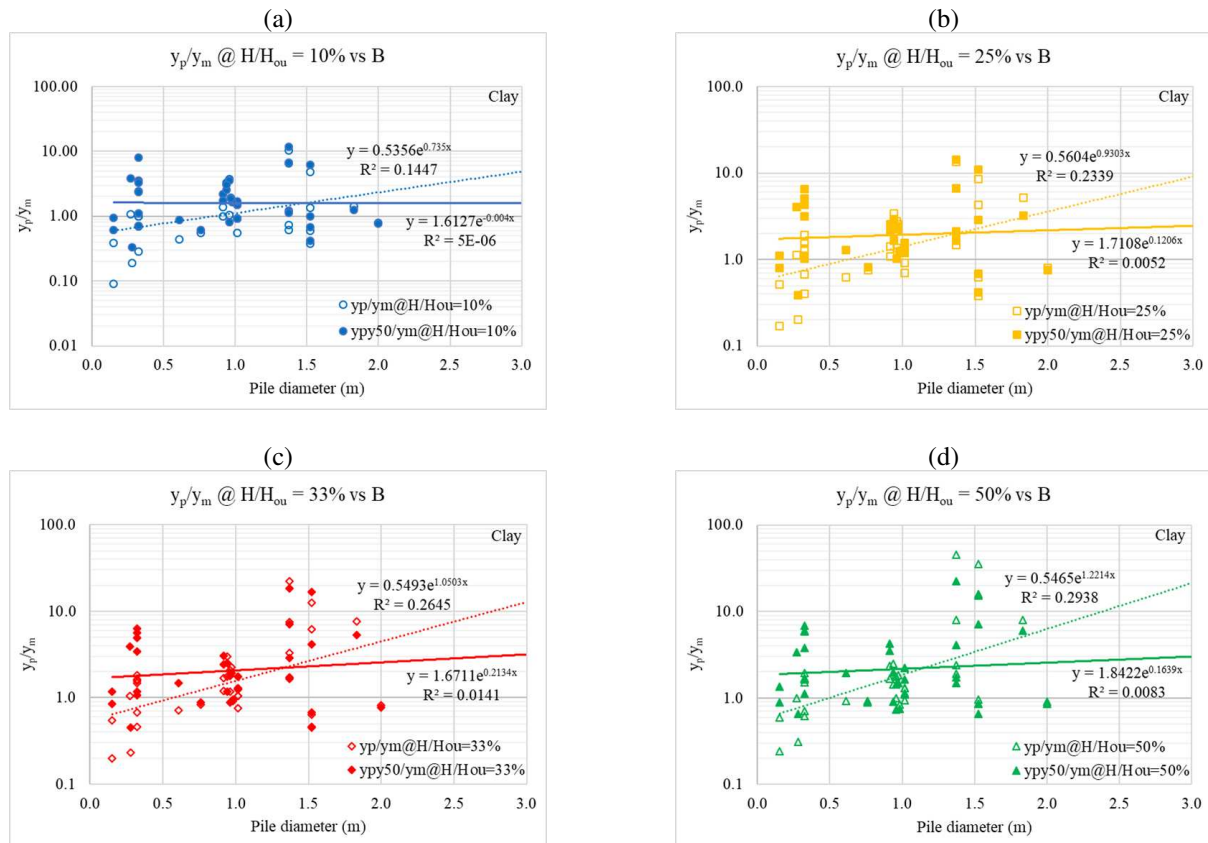


Figure 22. Ratio of Predicted over Measured Deflection versus Pile Diameter at Applied Loads Equal to (a) 10, (b) 25, (c) 33, and (d) 50 Percent of the Ultimate Lateral Load Before and After the Proposed Modification in Clay. In the Legend,  $y_p$  is the Predicted Deflection Before Correction and  $y_{p50}$  is the Predicted Deflection After Correction.

## PROBABILISTIC ANALYSES

The prediction of pile deflection under lateral loading exhibits uncertainty. This is exemplified by the scatter plot of predicted vs. measured deflection at 10% of the ultimate lateral load (Fig. 23(a)). In this case, one can count the number  $n$  of points on the graph for which the predicted value is less than the measured value. For Fig. 23(a) the value of  $n$  is 1. Since there is a total of 35 points on the graph, the probability that the deflection will be underpredicted according to this data is  $1/35 = 0.0286$  or 2.86%. If one decides to multiply all predicted value by a constant  $\theta$  equal to 0.5, for example, then the number of cases where the deflection would be underpredicted would increase to 19 (Fig. 23(b)) and the probability of underpredicting would be  $19/35 = 0.5429$  or 54.29%. If, on the other hand, one multiplies all predicted values by a constant  $\theta$  equal to 2, then the number of underpredicted values becomes zero and so does the probability. This experimental way of defining the probability of underpredicting the deflection leads to a plot of the probability of underpredicting as a function of the prediction multiplier  $\theta$ .

$$y_{p\text{-prob}} = \theta y_{p\text{-det}} \quad (11)$$

Where  $y_{p\text{-prob}}$  is the probabilistically predicted deflection,  $\theta$  is the prediction multiplier function of the chosen probability of underpredicting, and  $y_{p\text{-det}}$  is the deterministic prediction using LPILE. Fig. 24 shows plots of the probability of underprediction PoU vs. the prediction multiplier  $\theta$ . For example, in Fig. 20, which refers to piles in sand, a multiplier equal to 1 would give a 6% probability that the predicted deflection would be smaller than the measured deflection. Fig. 25 shows the same plot for piles in clay; in this case, a multiplier equal to 2 seems necessary to obtain a 10% probability of underpredicting the measured deflection. Note that in Figs. 24 and 25, the predicted deflections correspond to using LPILE as is and before any of the improvements proposed in this article. Figs. 26 and 27 show the same graphs for the predicted deflection after including the proposed improvements.

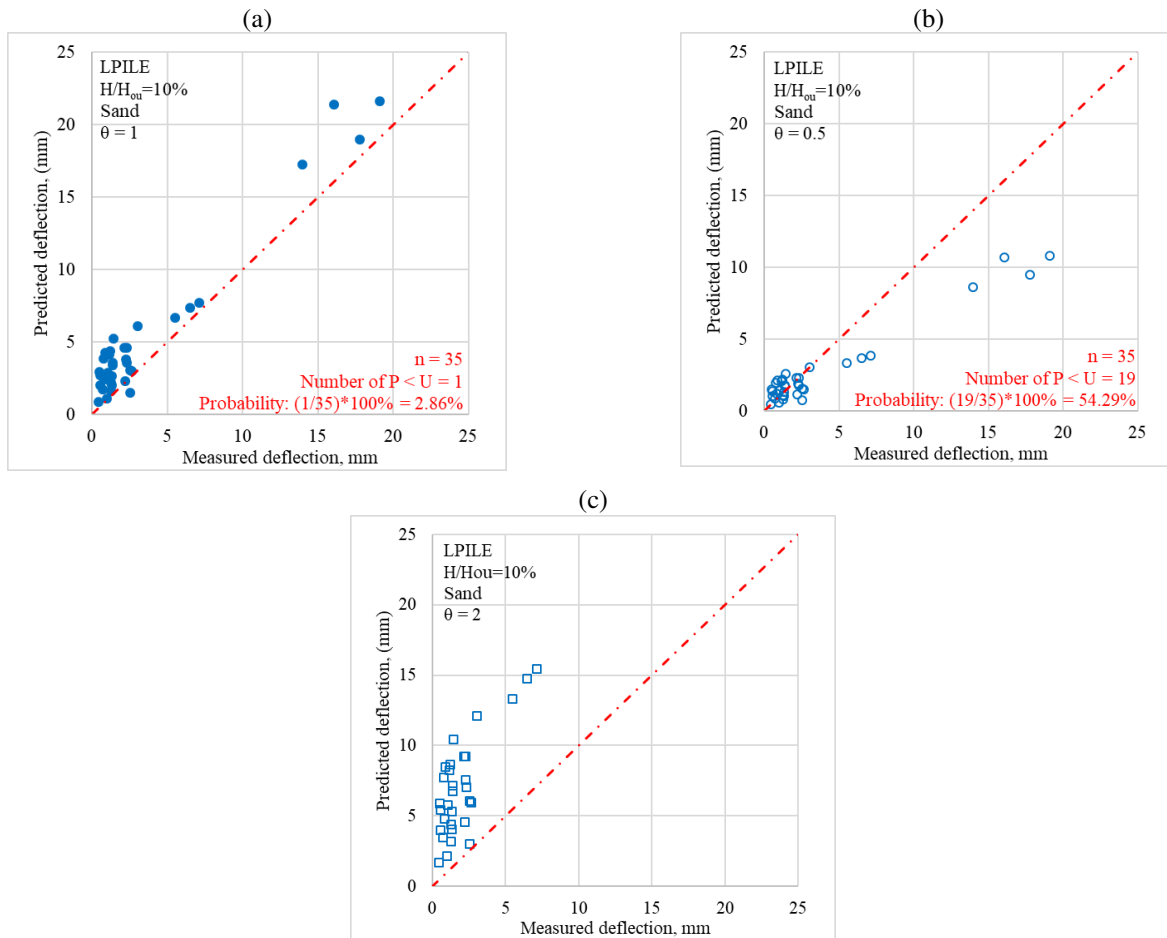


Figure 23. Comparison between Predicted and Measured Deflections for (a)  $\theta = 1.0$ , (b)  $\theta = 0.5$ , and (c)  $\theta = 2.0$  at  $H/H_{ou} = 10\%$  in Sand.

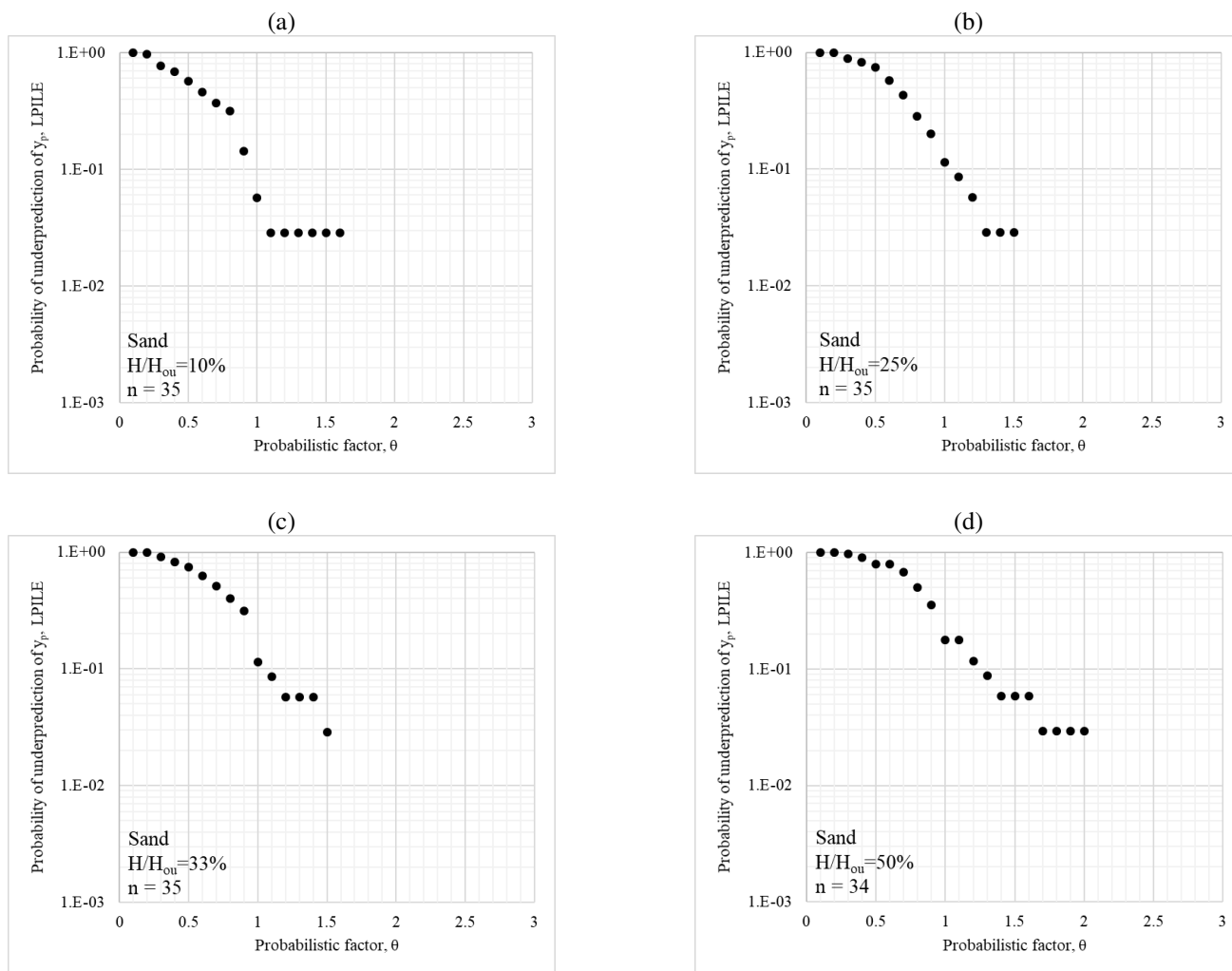


Figure 24. Probability of Underpredicting the Deflection Using LPILE at  $H/H_{ou}$  Equal to (a) 10, (b) 25, (c) 33, and (d) 50 Percent in Sand Before the Modification.

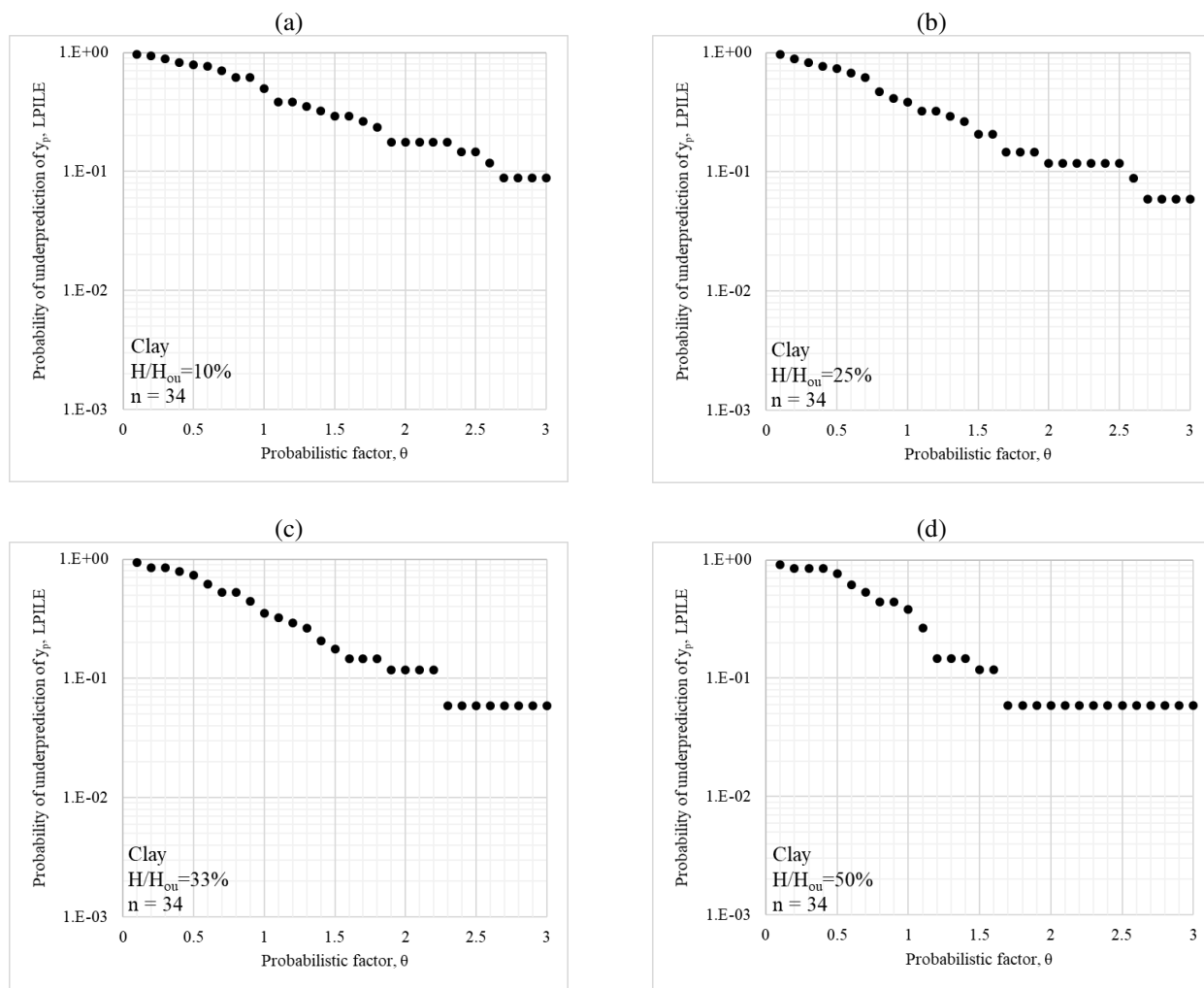


Figure 25. Probability of Underpredicting the Deflection Using LPILE at  $H/H_{ou}$  Equal to (a) 10, (b) 25, (c) 33, and (d) 50 Percent in Clay Before the Modification.

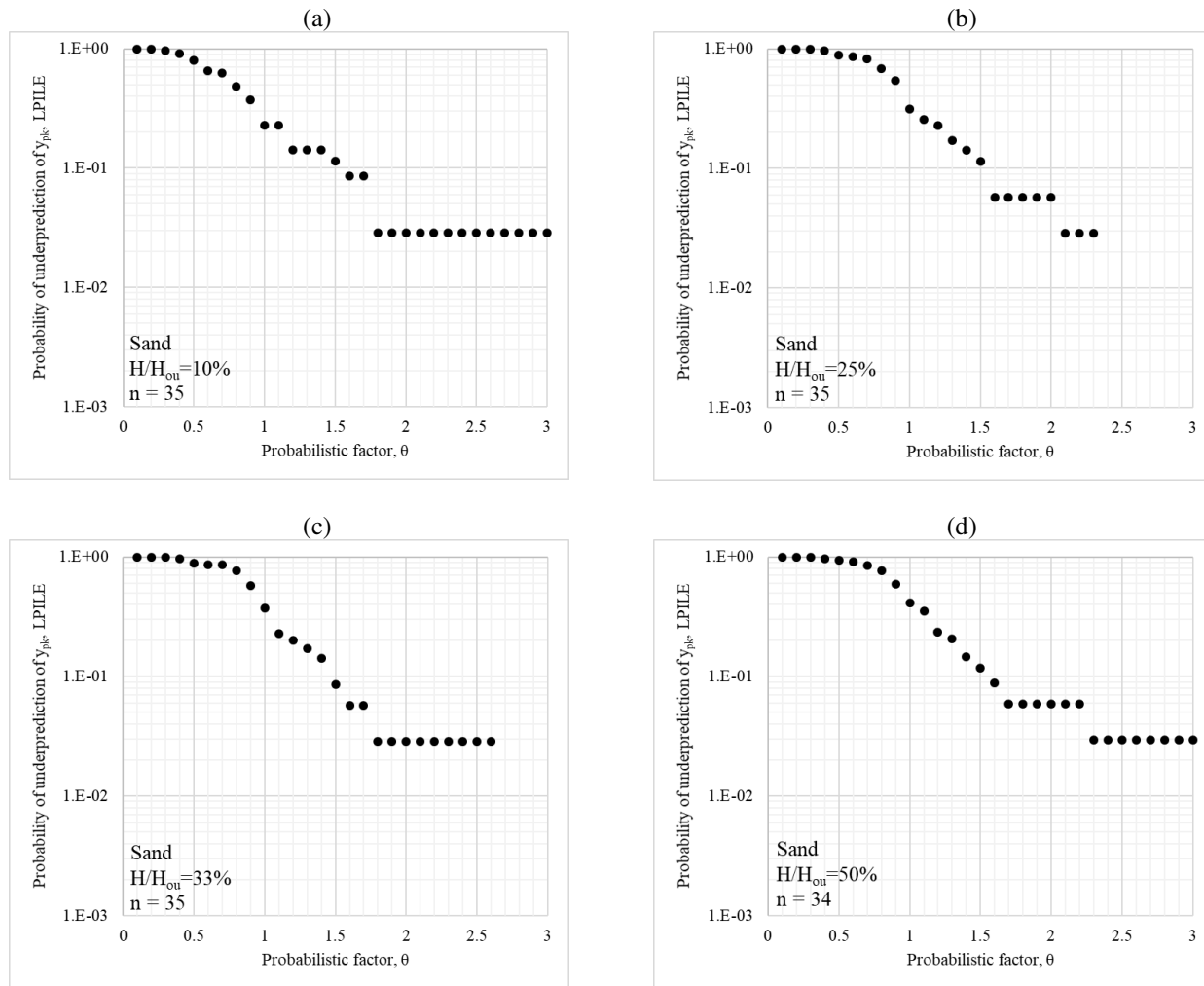


Figure 26. Probability of Underpredicting the Deflection Using LPILE at  $H/H_{ou}$  Equal to (a) 10, (b) 25, (c) 33, and (d) 50 Percent in Sand After the Modification.

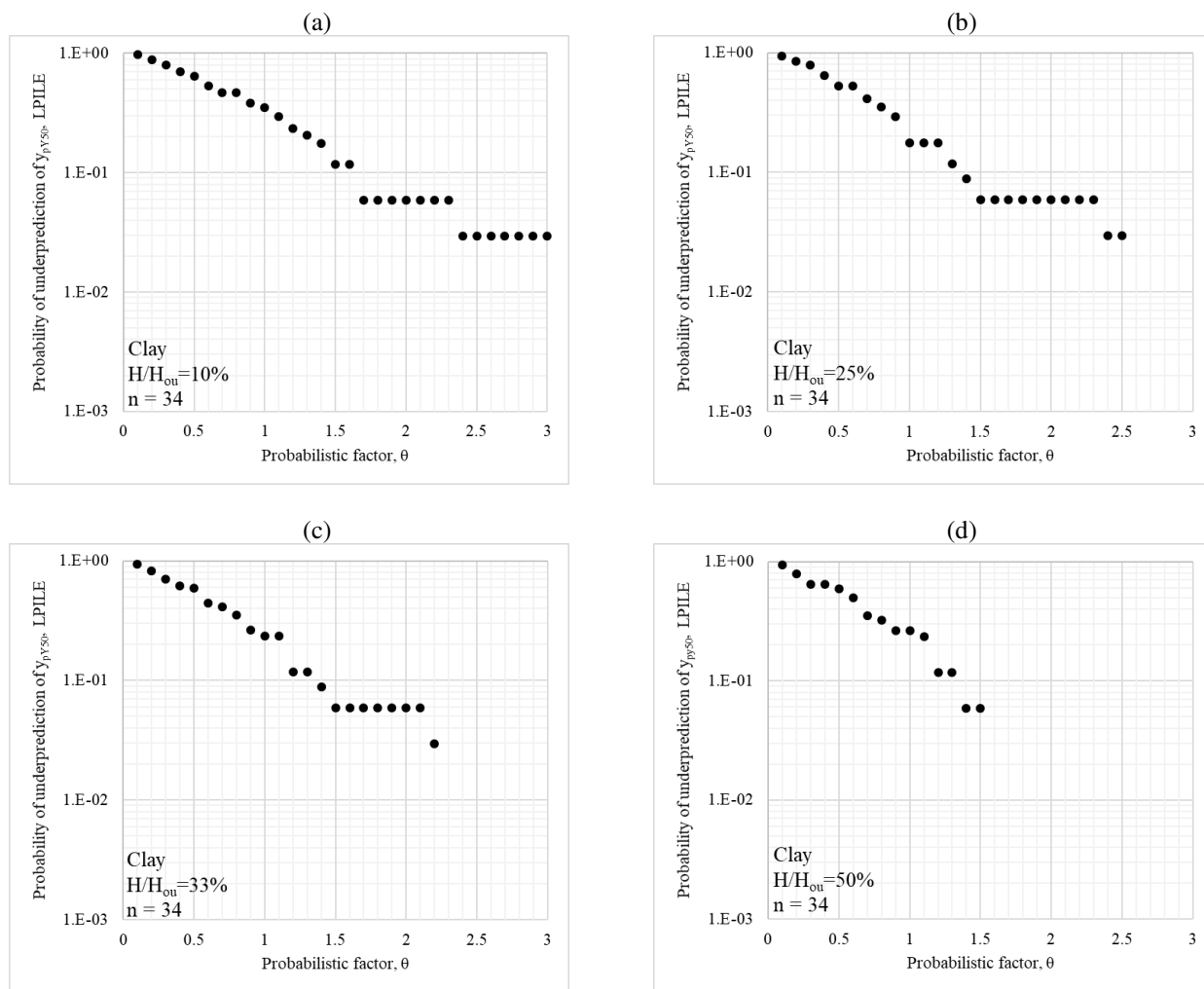


Figure 27. Probability of Underpredicting the Deflection Using LPILE at  $H/H_{ou}$  Equal to (a) 10, (b) 25, (c) 33, and (d) 50 Percent in Clay After the Modification.

## CONCLUSION

A database of 110 horizontal pile load tests was collected and organized in a spreadsheet called TAMU-Lateral, which is available upon request. The load tests were monotonic loading tests and gave a horizontal load vs. horizontal deflection curve for each test. Additional data was collected, including pile and soil information. There were 63 pile tests in sand and 47 pile tests in clay. In the end and because of various limitations in the collected data, a total of 69 load tests were used to evaluate the prediction. The pile diameter varied from 0.3 m to 3.0 m with about 42% of the pile diameters being larger than 1.5 m. The data came primarily from the United States but also from 8 other countries. For each load test case, the horizontal load vs. horizontal deflection curve was predicted using the program LPILE and compared to the measured curve.

The evaluation of the predictions took place along two main comparisons: a comparison between the predicted load  $L_p$  and the measured load  $L_m$  at given deflections of 1, 2, 5, and 10% of the pile diameter, and a comparison between the predicted deflection  $y_p$  and the measured deflection  $y_m$  at percentages of the ultimate lateral load equal to 10, 25, 33, and 50%. The ultimate lateral load was defined as the load corresponding to a horizontal deflection equal to 10 percent of the pile diameter. This deflection was not always reached in the load tests; in those cases, a hyperbolic extrapolation was used. For 35 of the 63 tests in sand, and for 34 of the 47 tests in clay, the extrapolation was either not needed or considered reasonable. These 35 tests in sand and 34 tests in clay entailed the database used in the evaluation of the deflection and load predictions.



The predictions were made using the program LPILE and the P-y criteria developed by API in sand (2010), Matlock in soft clay (1970) and Reese et al. in stiff clay (1974). The following conclusions are reached:

1. In sand, on average the loads are slightly underpredicted and the predicted load over measured load ratio,  $L_p/L_m$ , increases with pile diameter. The average  $L_p/L_m$  is 0.88 for all piles and increases with diameter from 0.79 for smaller diameter piles to 1.06 for larger diameter piles. Overall,  $L_p/L_m$  is between 0.28 and 2.42.
2. In sand, on average the deflections are significantly overpredicted and the predicted deflection over measured deflection ratio  $y_p/y_m$  decreases with the pile diameter. The average  $y_p/y_m$  is 1.75 for all piles and decreases with diameter from 1.91 for smaller diameter piles to 1.45 for larger diameter piles. Overall,  $y_p/y_m$  is between 0.29 and 6.02.
3. In clay, on average the loads are close to the measurements and the predicted load over measured load ratio  $L_p/L_m$  decreases with pile diameter. The average  $L_p/L_m$  is 0.97 for all piles and decreases with diameter from 1.02 for smaller diameter piles to 0.73 for larger diameter piles. Overall,  $L_p/L_m$  is between 0.32 and 2.67.
4. In clay, on average the deflections are significantly overpredicted and the predicted deflection over measured deflection ratio  $y_p/y_m$  increases with pile diameter. The average  $y_p/y_m$  is 2.75 for all piles and increases with diameter from 2.27 for smaller diameter piles to 4.96 for larger diameter piles. Overall, the ratio  $y_p/y_m$  is between 0.09 and 45.13.
5. The pile length to diameter ratio  $L/B$  has no significant influence on the predicted over measured deflection ratio  $y_p/y_m$  except for  $L/B$  values less than about 5, where the deflections are significantly overpredicted; this is attributed to the need to include other resistance to overturning such as base shear, base moment, and side shear. This is the topic of another publication by the authors.
6. The pile installation, including bored piles and driven piles, did not have any significant influence on the predicted over measured deflection ratio  $y_p/y_m$  within the range of diameter where the comparison was possible.

Two modifications are proposed to minimize the influence of the pile diameter on the predictions. Both are rooted in the stiffness of the P-y curves. In sand, the correction is associated with the modulus of subgrade reaction; in clay, the correction is associated with the increase in modulus vs. depth. They are:

|         |                          |  |
|---------|--------------------------|--|
| In sand | $k_{mod} = n_k k$        | with $n_k = 3$ for $B \leq 1m$<br>and $n_k = 3/B$ for $B > 1m$ |
| In clay | $y_{50mod} = n_y y_{50}$ | with $n_y = 0.72 \left(\frac{B}{B_0}\right)^{-0.7}$            |

The two modifications lead to a much-reduced dependence of the deflection ratio  $y_p/y_m$  on the pile diameter. Finally, the uncertainty associated with the deflection predictions is presented in a probabilistic way so that the engineer can make an educated decision on the level of probability he/she wishes to use in making the deflection predictions.

## ACKNOWLEDGMENTS

The first part of this project was funded by the Texas Department of Transportation Project 0-6956, where the project director was Chris Glancy, and the members of the project monitoring committee were John Delphia, David Fish, Justin Thomey, and Marie Fisk. The second part of the project was funded by the Spencer J. Buchanan Chair at Texas A&M University. The third part of the project was sponsored by Ensoft in Austin, where Shin-Tower Wang and Gonzalo Vasquez were the technical contacts. Many people contributed data to the database, including: Anne Lemnitzer, Associate Professor at the University of California at Irvine; John Hayes, Regional Sales Director at Aesculap Spine; Mohamed Ashour, Associate Professor at Alabama A&M University; Billy Camp, Technical Principal/Vice President at S&ME, Inc.; Raymond Castelli, Technical Director, Geotechnical Engineering at WSP; Jon Sinnreich, Principal Engineer at Load Test Consulting (LTC); Ikuo Towhata, Director at Tohata Architects & Engineers (Professor Emeritus, University of Tokyo); James Long, Emeritus Professor at University of Illinois Department of Civil Engineering; John Turner, Senior Principal Engineer at Dan Brown & Associates; Dan Brown, President/Senior Principal Engineer at Dan Brown & Associates; and Igor Kolibin, Director of NIIOSP in Moscow. Undergraduate students Kathryn Jennings and Rachel Holzhauser assisted with many of the figures.



---

## REFERENCES

API. (2010). *Recommended Practice for Planning, Designing and Constructing Fixed Offshore Platforms - Working Stress Design*, API RP 2A-WSD.

Ahmed, S. S., and Hawlader, B. (2016). "Numerical analysis of large-diameter monopiles in dense sand supporting offshore wind turbines." *International Journal of Geomechanics*, 16(5), 04016018.

Ashour, M., Norris, G., and Pilling, P. (2002). "Strain wedge model capability of analyzing behavior of laterally loaded isolated piles, drilled shafts, and pile groups." *Journal of Bridge Engineering*, 7(4), 245-254.

Banerjee, P. K., and Davies, T. G. (1978). "The behaviour of axially and laterally loaded single piles embedded in nonhomogeneous soils". *Geotechnique*, 28(3), 309-326.

Briaud, J. L. (2013). *Geotechnical engineering: unsaturated and saturated soils*, John Wiley & Sons.

Briaud, J. L., and Wang, Y. C. (2018). *Synthesis of Load-Deflection Characteristics of Laterally Loaded Large Diameter Drilled Shafts: Technical Report (No. FHWA/TX-18/0-6956-R1)*.

Broms, B. B. (1964). "Lateral resistance of piles in cohesive soils." *Journal of the Soil Mechanics and Foundations Division*, 90(2), 27-64.

Broms, B. B. (1964). "Lateral resistance of piles in cohesionless soils." *Journal of the Soil Mechanics and Foundations Division*, 90(3), 123-158.

Byrne, B. W., McAdam, R. A., Burd, H. J., Houlsby, G. T., Martin, C. M., Gavin, K., ... and Potts, D. M. (2015). *Field testing of large diameter piles under lateral loading for offshore wind applications*.

Comodromos, E. M., and Pitilakis, K. D. (2005). "Response evaluation for horizontally loaded fixed-head pile groups using 3-D non-linear analysis." *International Journal for Numerical and Analytical Methods in Geomechanics*, 29(6), 597-625.

Hansen, J. B. (1961). "The ultimate resistance of rigid piles against transversal forces". *Bulletin 12, Danish Geotech. Institute*, 1-9.

Isenhower, W. M., Wang, S.T., and Vasquez, L. G. (2018). *Technical Manual for LPile 2018*.

Jeanjean, P. (2009). "Re-assessment of py curves for soft clays from centrifuge testing and finite element modeling. In Offshore Technology Conference. Offshore Technology Conference.

Matlock, H. (1970). "Correlations for design of laterally loaded piles in soft clay". *Offshore Technology in Civil Engineering Hall of Fame Papers from the Early Years*, 77-94.

McClelland, B. (1956). "Soil modulus for laterally loaded piles." *Journal of the Soil Mechanics and Foundations division*, 82(4), 1-22.

Poulos, H. G. (1971). "Behavior of laterally loaded piles I. single piles." *Journal of Soil Mechanics & Foundations Div.*

Randolph, M. F. (1981). "The response of flexible piles to lateral loading." *Geotechnique*, 31(2), 247-259.

Randolph, M. F., and Houlsby, G. T. (1984). "The limiting pressure on a circular pile loaded laterally in cohesive soil." *Geotechnique*, 34(4), 613-623.

Reese, L. C. (1958). "Discussion on soil modulus for laterally loaded piles." *Trans. ASCE*, 123, 1071-1074.

Reece, L. C., Cox, W., and Koop, F. (1975). "Field testing and analysis of laterally loaded piles in stiff clay." *Proc. 7th offshore technology conference*, 2, 671-690.

Reese, L. C., and Welch, R. C. (1975). "Lateral loading of deep foundations in stiff clay." *Journal of Geotechnical and Geoenvironmental Engineering*, 101.

Reese, L. C., Cox, W. R., and Koop, F. D. (1974). "Analysis of laterally loaded piles in sand." *Offshore Technology in Civil Engineering Hall of Fame Papers from the Early Years*, 95-105.

Stevens, J., and Audibert, J. (1979). "Re-examination of py curve formulations." *Offshore technology conference*.

Wang Y.C., Briaud, J. L., Wang S.T., and Vasquez G. (2022). "Large Diameter Piles Subjected to Lateral Forces: Tip and Side Resistances." *Geo-Congress 2022: Foundations, Soil Improvement, and Erosion*, Reston, VA: American Society of Civil Engineers.

Zhang, L., and Ahmari, S. (2013). "Nonlinear analysis of laterally loaded rigid piles in cohesive soil." *International Journal for Numerical and Analytical Methods in Geomechanics*, 37(2), 201-220.

Zhang, Y., Andersen, K. H., and Tedesco, G. (2016). "Ultimate bearing capacity of laterally loaded piles in clay—Some practical considerations." *Marine Structures*, 50.



INTERNATIONAL JOURNAL OF  
**GEOENGINEERING  
CASE HISTORIES**

*The Journal's Open Access Mission is  
generously supported by the following Organizations:*



Geosyntec  
consultants

engineers | scientists | innovators

**CONE**TEC



**ENGEO**  
Expect Excellence

Access the content of the ISSMGE International Journal of Geoengineering Case Histories at:  
<https://www.geocasehistoriesjournal.org>